



## 저작자표시-비영리-변경금지 2.0 대한민국

이용자는 아래의 조건을 따르는 경우에 한하여 자유롭게

- 이 저작물을 복제, 배포, 전송, 전시, 공연 및 방송할 수 있습니다.

다음과 같은 조건을 따라야 합니다:



저작자표시. 귀하는 원저작자를 표시하여야 합니다.



비영리. 귀하는 이 저작물을 영리 목적으로 이용할 수 없습니다.



변경금지. 귀하는 이 저작물을 개작, 변형 또는 가공할 수 없습니다.

- 귀하는, 이 저작물의 재이용이나 배포의 경우, 이 저작물에 적용된 이용허락조건을 명확하게 나타내어야 합니다.
- 저작권자로부터 별도의 허가를 받으면 이러한 조건들은 적용되지 않습니다.

저작권법에 따른 이용자의 권리는 위의 내용에 의하여 영향을 받지 않습니다.

이것은 [이용허락규약\(Legal Code\)](#)을 이해하기 쉽게 요약한 것입니다.

[Disclaimer](#)

# The role of polaprezinc in fracture healing by differentiation of both osteoclasts and osteoblasts

Yoo Jung Park

Department of Medicine

The Graduate School, Yonsei University

# The role of polaprezinc in fracture healing by differentiation of both osteoclasts and osteoblasts

Directed by Professor Jin Woo Lee

The Doctoral Dissertation  
submitted to the Department of Medicine,  
the Graduate School of Yonsei University  
in partial fulfillment of the requirements for the degree of  
Doctor of Philosophy in Medical Science

Yoo Jung Park

December 2022

This certifies that the Doctoral Dissertation of  
Yoo Jung Park is approved.

-----  
Thesis Supervisor : Jin Woo Lee

-----  
Thesis Committee Member#1 : Sahng Wook Park

-----  
Thesis Committee Member#2 : Jae Myun Lee

-----  
Thesis Committee Member#3: Jae-Hyuck Shim

-----  
Thesis Committee Member#4: Kwang Hwan Park

The Graduate School  
Yonsei University

December 2022

## ACKNOWLEDGEMENTS

I would like to thank everyone who has given great helps to complete this work.

Firstly, I'd like to express my sincere gratitude to the thesis supervisor, Prof. Jin Woo Lee, for providing guidance and feedback throughout this work. His immense knowledge and plentiful experience have encouraged me in all the time of my academic and daily life. I would also like to thank Prof. Sahng Wook Park, Prof. Jae Myun Lee, Prof. Jae-Hyuck Shim and Prof. Kwang Hwan Park for their invaluable supervision, support and tutelage during the course of my degree.

I really thank you Prof. Dong Suk Yoon, Prof. Kyoung-Mi Lee, Eun Ae Ko and other staffs in LJWOS lab, the Department of Orthopaedic Surgery in Yonsei University College of Medicine, for their continual support, guidance and academic advice from the whole faculty.

Most of all, I express my deepest gratitude to my wife Jung Hyun Lee, daughter Seo Ah Park, my mother and father, for their unfailing support and continuous encouragement.

## <TABLE OF CONTENTS>

ABSTRACT .....	iv
I. INTRODUCTION .....	1
II. MATERIALS AND METHODS .....	3
1. Cell culture and reagents .....	3
2. Cell viability measurement .....	4
3. <i>In vitro</i> osteogenic differentiation .....	4
4. Alkaline phosphatase and alizarin red S staining .....	4
5. <i>In vitro</i> osteoclastogenic differentiation .....	5
6. TRAP activity and TRAP staining .....	5
7. Quantitative real-time polymerase chain reaction .....	6
8. Western blot analysis .....	8
9. Intracellular zinc measurement .....	8
10. Luciferase assay .....	9
11. siRNA-mediated knockdown .....	9
12. Mouse femoral fracture model .....	9
13. Micro-computed tomography .....	10
14. Immunohistochemical analysis .....	11
15. Immunocytochemistry .....	11
16. Protein fractionation .....	12
17. Statistics and reproducibility .....	12
III. RESULTS .....	13
1. Polaprezinc promotes osteoblast differentiation in hBMSCs .....	13
2. Polaprezinc accelerates osteoclast differentiation in mBMMs .....	22
3. Different effects of polaprezinc and zinc on osteoblast and osteoclast differentiation .....	25
4. YAP may be as responsible molecular mediator of polaprezinc-induced osteoblast and osteoclast activity .....	28

5. Oral administration of polaprezinc accelerates bone remodeling in a mouse fracture model .....	35
IV. DISCUSSION .....	42
V. CONCLUSION .....	44
REFERENCES .....	45
ABSTRACT (IN KOREAN) .....	53
PUBLICATION LIST .....	55

## LIST OF FIGURES

Figure 1. Schematic of the study and effects of polaprezinc on the osteogenic differentiation of hBMSCs .....	17
Figure 2. L-carnosine does not affect osteoblast and osteoclast differentiation .....	21
Figure 3. Effects of polaprezinc on the osteoclast differentiation of mBMMs .....	24
Figure 4. Comparative study of polaprezinc and zinc sulfate differentiation into osteoblast and osteoclast lineages .....	27
Figure 5. Knockdown study of YAP in polaprezinc-treated hBMSCs and RAW264.7 cells .....	34
Figure 6. Micro-CT analysis in a mouse femoral fracture model and the effects of polaprezinc .....	41

## LIST OF TABLES

Table 1. Real-time PCR thermal cycling profile .....	6
Table 2. Primers sequences used for qRT-PCR .....	7

## ABSTRACT

### **The role of polaprezinc in fracture healing by differentiation of both osteoclasts and osteoblasts**

Yoo Jung Park

*Department of Medicine  
The Graduate School, Yonsei University*

(Directed by Professor Jin Woo Lee)

Fractures and fracture related complications are common causes of morbidity and mortality nowadays. According to the data from National Health Insurance and Assessment Service, over 2,200,000 fractures are sustained every year in South Korea of all ages and sexes. Although the majority heal satisfactorily, 5% to 10% go on to delayed union or non-union. Vitamin D and calcium are the broadly available medications for fracture healing, while zinc has been recognized as a nutritional supplement for healthy bones. We aimed to use polaprezinc, an anti-ulcer drug and a chelate form of zinc and L-carnosine, as a supplement for fracture healing.

To investigate whether polaprezinc could be a candidate small molecule for drug repurposing to bone-related diseases, we used hBMSCs and mBMMs to determine whether polaprezinc acts as a positive or negative modulator during osteoblast and osteoclast differentiation. Next, we confirmed the effects of polaprezinc on hBMSC differentiation to osteogenic lineage at the early and late stages of differentiation. We compared the mRNA levels of osteogenic-related genes between vehicle- and polaprezinc-treated hBMSCs. To clarify the effect of polaprezinc on osteoclast

differentiation, mBMMs were induced by treatment with mRANKL in the presence of polaprezinc dose dependently. To evaluate whether polaprezinc may serve as a supplement for enhancing the treatment of fracture healing, mice with femoral fractures were employed for animal studies in vivo.

Polaprezinc enhanced expression of osteogenesis-related genes and enhanced osteogenic potential of human bone marrow-derived mesenchymal stem cells such as RUNX2 protein level and the osteoclast differentiation potential of mouse bone marrow-derived monocytes such as TRAP activities induced by RANKL. In mouse experimental models with bone fractures, oral administration of polaprezinc accelerated fracture healing and maintained a high number of both osteoblasts and osteoclasts in the fracture areas.  $\mu$ CT image showed polaprezinc group had lower remaining callus volume and callus BMD was significantly increased in orally administered polaprezinc mice.

In conclusion, polaprezinc promotes the fracture healing process efficiently by enhancing the activity of both osteoblasts and osteoclasts. Therefore, these data suggest that drug repositioning of polaprezinc as a fracture healing therapy would be helpful for patients with fractures.

---

Key words : polaprezinc, osteoblast, osteoclast, fracture healing, drug repositioning

## **The role of polaprezinc in fracture healing by differentiation of both osteoclasts and osteoblasts**

Yoo Jung Park

*Department of Medicine  
The Graduate School, Yonsei University*

(Directed by Professor Jin Woo Lee)

### **I. INTRODUCTION**

Zinc is an essential element that functions as a structural component in the human body, playing important roles in several biological processes, including DNA to protein synthesis<sup>1</sup>. Zinc is relatively abundant in skeletal tissues, such as bone, cartilage, and teeth<sup>2</sup>, and zinc deficiency is known to delay bone growth and increase skin fragility<sup>3</sup>. Interestingly, research has shown that zinc supplementation has positive effects on bone health, including maintaining bone mineral density and accelerating fracture healing<sup>4,5</sup>. In addition, zinc has been shown to stimulate the proliferation and differentiation of osteoblasts by stimulating collagen synthesis to improve bone formation<sup>6,7</sup>; along with vitamin C and copper, zinc is regarded as an important cofactor for collagen production<sup>8</sup>, wherein zinc activates proteins responsible for collagen synthesis and zinc deficiency reduces that the amount of collagen produced<sup>9</sup>. Previous studies have demonstrated that zinc acts a signaling molecule in various intracellular signaling pathways<sup>10,11</sup>, and our research has indicated that zinc is involved in the calcium-calcineurin-NFATc1 signaling pathway to inhibit osteoclast differentiation in mouse bone marrow-derived monocytes (mBMMs), as well as the AMP-PKA-CREB signaling pathway to promote osteoblast differentiation in human bone marrow-derived mesenchymal stem cells (hBMSCs)<sup>12,13</sup>. We suspect that zinc may be involved in more intracellular signaling pathways. Therefore, in order to properly apply zinc to bone-related diseases, links between zinc and various signaling pathways need to

be established.

Zinc is also known to be efficacious for the repair of damaged tissue and has been shown to protect against gastric ulceration<sup>15</sup>. Polaprezinc is an oral bioavailable chelate consisting of zinc and L-carnosine with potential gastrointestinal protection, and antioxidant, anti-ulcer, and anti-inflammatory properties<sup>14-17</sup>. In clinical trials, polaprezinc was applied as a replacement therapy for zinc deficiency<sup>18</sup>. As zinc deficiency interferes with fracture healing<sup>19</sup>, polaprezinc administration may also be considered a potential therapeutic agent to improve bone regeneration or increase the effectiveness of fracture-related disease treatment. The combination or chelation of zinc and carnosine, which results in polaprezinc, has superior health benefits compared to individual treatment as carnosine enhances the absorption of zinc because of its solubility and that it possibly delivers zinc to the tissues in a delayed and extended release manner<sup>20,21</sup>. The chemical reaction of polaprezinc has been shown to release zinc during intestinal absorption *in vivo*<sup>22</sup>. This means that polaprezinc dissociate into L-carnosine and zinc during intestinal absorption<sup>23</sup>. Since polaprezinc is dissolvable in acid and appears to protect mucosal lesions, it can be thought that polaprezinc dissociates into two compounds during intestinal absorption<sup>24</sup>. Hydrochloric acid (HCl) solution is mainly used to dissolve polaprezinc in *in vitro* experiments, which means that the *in vitro* delivery method of polaprezinc by acidic solution makes it possible to dissociate polaprezinc into L-carnosine and zinc to mimic *in vivo* conditions. Therefore, *in vitro* experiments with polaprezinc may be suitable to study changes *in vivo* following oral administration. However, to date, there have been no reports on whether the oral administration of polaprezinc has a positive effect on fracture healing, as well as modulating the molecular mechanisms for osteoblast and osteoclast homeostasis *in vitro*.

Previous studies show pharmacokinetic characteristic of polaprezinc. Intestinal absorption of polaprezinc was studied in rats using <sup>14</sup>C- and <sup>65</sup>Zn-labeled compounds<sup>22</sup>. Polaprezinc was suggested to dissociate to its components, L-carnosine and zinc, during intestinal absorption. After a single administration of <sup>14</sup>C-labeled polaprezinc to rats, the

accumulated excretion rates of polaprezinc were 4.1% in urine, 13.3% in feces, and 38.8% in exhalation. For  $^{65}\text{Zn}$ -labeled polaprezinc, the excretion rates were 0.3% in urine and 85.0% in feces. The absorption rate of Zn was estimated to be 11%.

Drug repositioning is a way to investigate exiting drugs or molecules for other therapeutic purposes and can be a strategy for identifying new uses for approved drugs that are beyond the scope of their intended use<sup>25</sup>. Utilizing drug repositioning can minimize expensive and time-consuming processes for identifying new indications for drugs that have already been approved for patient use. In this study, we employed polaprezinc as a strategy for drug repositioning. We showed that polaprezinc enhanced the differentiation potential of hBMSCs and mBMMs into osteoblasts and osteoclasts, respectively. Polaprezinc treatment upregulated the protein level of the yes-associate protein (YAP), which is a positive regulator of osteoblast and osteoclast differentiation, in precursors of osteoblasts and osteoclasts, respectively. In the study of mice with bone fractures, the oral administration of polaprezinc enhanced fracture healing. Our results indicate that polaprezinc is a potential supplement for fracture healing.

## II. MATERIALS AND METHODS

### Cell culture and reagents

This study was approved by the Institutional Review Board (IRB) of Yonsei University College of Medicine (No: 4-2017-0232). Bone marrow aspirates were obtained from the posterior iliac crests of seven adult donors (55-65 years old). MSCs isolated from human bone marrow were selected based on their ability to adhere to plastic cell culture flasks, and >98% of the cultured cells were positive for CD90 and CD105, but negative for CD34 and CD45<sup>26</sup>. hBMSCs were maintained in low-glucose Dulbecco's modified Eagle's medium (DMEM-LG; Gibco, Grand Island, NY, USA) supplemented with 10% fetal bovine serum (FBS, Gibco, Grand Island, NY, USA) and 1% antibiotic-antimycotic solution (Gibco, Grand Island, NY, USA) and were used within five passages. RAW264.7 cells (Korean Cell Line Bank, Seoul, South Korea) were maintained in high-glucose

DMEM (Gibco, Grand Island, NY, USA) supplemented with 10% FBS (Gibco, Grand Island, NY, USA) and 1% antibiotic-antimycotic solution (Gibco, Grand Island, NY, USA). mBMMs were cultured in  $\alpha$ -minimum essential medium (Gibco, Grand Island, NY, USA) containing 10% FBS and 1% antibiotic-antimycotic solution. Polaprezinc (CAS 107667-60-7, Santa Cruz Biotechnology, Santa Cruz, CA, USA) was dissolved in 1 M hydrogen chloride and used at a final concentration of 50  $\mu$ M. ZnSO<sub>4</sub> was purchased from Sigma-Aldrich (Saint Louis, MO, USA).

#### **Cell viability measurement**

Cell viability was assessed to measure the cytotoxicity of polaprezinc. hBMSCs were seeded in 12-well culture plates at a density of  $1 \times 10^4$  cells/well. The cells were then maintained in growth media and the media were changed every two days with different concentrations of polaprezinc or ZnSO<sub>4</sub> for 14 days. To measure the levels of cell viability, Ez-Cytox (tetrazolium salts, DoGen, Seoul, Korea) reagent was added to each well and incubated for 2 hr at 37°C. Cell viability was measured at 450 nm using a microplate reader (VersaMax™ Microplate Reader, CA, USA).

#### ***In vitro* osteogenic differentiation**

hBMSCs were seeded at  $8 \times 10^4$  cells/well in 12-well plates. To induce *in vitro* osteogenesis, hBMSCs were cultured in osteogenic medium [DMEM-LG containing 10% FBS, 1% antibiotic-antimycotic solution, 10 mM  $\beta$ -glycerophosphate (Sigma-Aldrich, Saint Louis, MO, USA), and 50  $\mu$ g/mL ascorbic acid (Gibco, Grand Island, NY, USA)] with or without polaprezinc or ZnSO<sub>4</sub> for 5–12 days. Polaprezinc- or ZnSO<sub>4</sub>-containing osteogenic medium was replaced every other day.

#### **Alkaline phosphatase and alizarin red S staining**

To confirm the differentiation activity of osteogenesis, we performed alkaline phosphatase (ALP) and alizarin red S staining. For ALP staining, the cells were fixed with citrate

buffer:acetone fixative (2:3). hBMSCs were stained using alkaline staining solution, which was mixed with 1.5mM fast blue RR salt solution (Sigma-Aldrich, Saint Louis, MO, USA) and 0.25% naphthol AS-MX phosphate alkaline solution 120  $\mu$ l (Sigma-Aldrich, Saint Louis, MO, USA) for 30 min. To measure ALP activity, hBMSCs were incubated with substrate solution containing 0.5 M  $\text{Na}_2\text{CO}_3$ , 0.5 M  $\text{NaHCO}_3$ , 1 M  $\text{MgCl}_2$ , and phosphatase substrate (Sigma-Aldrich, Saint Louis, MO, USA) for 30 min at room temperature. The absorbance of the substrate solution was measured at 405 and 450 nm. ALP activity was normalized to Alamar blue (Invitrogen, Carlsbad, CA, USA). For alizarin red S staining, differentiated hBMSCs were fixed in ice-cold 70% ethanol and stained with 2% alizarin red S solution. For quantification of alizarin red S staining, the cells were stained with 10% cetylpyridinium chloride and the absorbance was measured at 595 nm using a microplate reader.

#### ***In vitro* osteoclastogenic differentiation**

The femur and tibia were removed from 6-week-old male C57BL/6 mice. Cells derived from the bone marrow were collected and cultured in growth media containing M-CSF (10 ng/ml). After 24 hr, non-adherent cells were collected and seeded in a 100 mm dish and treated with M-CSF (30 ng/ml)<sup>12</sup>. After 48 hr, non-adherent cells were collected and cultured with 10 ng/mL mM-CSF (R&D Systems, Minneapolis, MN, USA). mBMMs were detached using Detachin™ (Genlantis, San Diego, CA, USA) and  $5 \times 10^4$  cells were seeded on 24-well plates for osteoclastogenesis. mBMMs were cultured in growth media containing 10 ng/mL mM-CSF and 10 ng/mL mRANKL (R&D Systems, Minneapolis, MN, USA) with or without polaprezinc. In addition, for inducing osteoclastic differentiation, RAW264.7 cells were plated at a concentration of 10,000 cells/well in a 24-well plate and treated with 50 ng/mL mRANKL in growth media with or without polaprezinc or  $\text{ZnSO}_4$ .

#### **TRAP activity and TRAP staining**

To evaluate TRAP activity, 50  $\mu$ L of osteoclast culture supernatant was incubated with a

substrate mix containing acetate solution (Sigma-Aldrich, Saint Louis, MO, USA), 1 M sodium tartrate, and phosphatase substrate (Sigma-Aldrich, Saint Louis, MO, USA) for 1 hr at 37°C. The reaction was stopped by adding 3 N HCl and measured at an absorbance wavelength of 405 nm. TRAP staining was performed using an Acid Phosphatase, Leukocyte kit (Sigma-Aldrich, Saint Louis, MO, USA) following the manufacturer's instructions. Cells were fixed with fixative solution and stained with staining solution for 1 hr at 37°C. TRAP-positive multinucleated cells containing more than five nuclei were considered as osteoclasts.

### Quantitative real-time polymerase chain reaction (qRT-PCR)

Total RNA was extracted using the RNeasy Mini Kit (Qiagen, Hilden, Germany) according to the manufacturer's instructions. Complementary DNA was synthesized using the Omniscript Reverse-Transcription Kit (Qiagen, Hilden, Germany) following the manufacturer's protocol. qRT-PCR was performed using 2 × qPCRBIO SyGreen Mix Hi-Rox (PCR Biosystems, London, UK). The PCR cycle durations and temperatures are outlined in Table 1 below. The specific primer sets (Bioneer, Daejeon, Korea) are shown in Table 2. *ALPL* (P324388) primer sets were purchased from Bioneer (Daejeon, Korea).

**Table 1. Real-time PCR thermal cycling profile**

Polymerase activation and DNA Denaturation	Amplification			Melt-Curve Analysis
	Denaturation	Annealing	Cycles	
95 °C/ 2min/1 cycle	95 °C/ 5 sec	60 °C/ 20 sec	35-40	60-95°C increment 2-5 sec/ step

**Table 2. Primers sequences used for qRT-PCR**

Gene	Primer sequence (5' → 3')
Human	
<i>RUNX2</i>	F: TACAAACCATACCCAGTCCCTGTTT
	R: AGTGCTCTAACCACAGTCCATGCA
<i>COL1A1</i>	F: GCCCTGCTGGAGAGGAAGGA
	R: GCCAGGGAAACCACGGCTAC
<i>SPP1</i>	F: CCGTTGCCCAGGACCTGAA
	R: TGTGGCTGTGGGTTTCAGCA
<i>IBSP</i>	F: ATACCATCTCACACCAGTTAGAATG
	R: AACAGCGTAAAAGTGTTTCCTATTTC
<i>BGLAP</i>	F: AGAGCCCCAGTCCCCTACCC
	R: AGGCCTCCTGAAAGCCGATG
<i>GAPDH</i>	F: CTGCTGATGCCCCCATGTTC
	R: ACCTTGGCCAGGGGTGCTAA
Mouse	
<i>Nfatc1</i>	F: GGTA ACTCTGTCTTTCTAACCTTAAGCTC
	R: GTGATGACCCCAGCATGCACCAGTCACAG
<i>Dcstamp</i>	F: TCCTCCATGAACAAACAGTTCCAA
	R: AGACGTGGTTTAGGAATGCAGCTC

<i>Ctsk</i>	F: AGGCAGCTAAATGCAGAGGGTACA
	R: ATGCCGCAGGCGTTGTTCTTATTC
<i>Gapdh</i>	F: GTGTTCCTACCCCAATGTGT
	R: ATTGTCATACCAGGAAATGAGCTT

### Western blot analysis

For immunoblotting, cells were lysed with ProPrep™ (iNtRON Biotechnology, Seongnam, Gyeonggi-do, Korea). Whole cell lysates were centrifuged at 13,000 rpm for 20 min at 4°C and quantified using a SMART™ BCA Protein Assay Kit (iNtRON Biotechnology, Seongnam, Gyeonggi-do, Korea). Protein samples were loaded onto SDS-PAGE gels and transferred to a polyvinylidene difluoride membrane (Amersham Pharmacia, Piscataway, NJ, USA). Western blot analysis was performed using primary antibodies against mouse anti-RUNX2 (Millipore, Burlington, MA, USA), rabbit anti-HSP90 (Santa Cruz Biotechnology, Dallas, TX, USA), rabbit anti-NFATc1 (Santa Cruz Biotechnology, Dallas, TX, USA), anti-yes-associated protein-1 (YAP; Cell Signaling, Danvers, MA, USA), anti-phosphoYAP<sup>S126</sup> (Cell Signaling, Danvers, MA, USA), and mouse anti-β-ACTIN (Santa Cruz Biotechnology, Dallas, TX, USA). ECL solution (Bio-Rad, Hercules, CA, USA) was used to visualize the signals. Relative band intensities were measured using ImageJ software (National Institutes of Health).

### Intracellular zinc measurement

Zinquin (Sigma-Aldrich, Saint Louis, MO, USA) was used to detect intracellular zinc levels after treatment with polaprezinc and ZnSO<sub>4</sub>. Briefly, polaprezinc and ZnSO<sub>4</sub> were applied to hBMSCs or RAW264.7 cells. After 24 hr, 25 μM Zinquin solution per well was dropped into the cell and incubated for 30 min at 37°C, and cells were washed three times with phosphate-buffered saline (PBS) to remove extracellular Zinquin. Fluorescence was measured at an excitation wavelength of 368 nm and emission of 490 nm using a Fluorometer (Varioskan Flash 3001, Thermo Fisher Scientific, Waltham, MA, USA).

### **Luciferase assay**

Cells were seeded in triplicate in six-well culture plates at  $1 \times 10^5$  cells and cultured for 24 hr, and the luciferase reporter assay was performed<sup>27</sup>. The cells were transfected with 500 ng of HOP-Flash (83467, Addgene) or HIP-Flash luciferase reporter plasmid (83466, Addgene) along with 10 ng of pRL-TK Renilla plasmid (Promega, Madison, WI, USA) using the Neon Transfection System (Invitrogen, Carlsbad, CA, USA) according to the manufacturer's instructions. The day after transfection, cells were treated with 50  $\mu$ M polaprezinc or ZnSO<sub>4</sub>, respectively. Luciferase and Renilla signals were measured 48 hr after transfection using a Dual Luciferase Reporter Assay Kit (Promega, Madison, WI, USA) according to the manufacturer's instructions.

### **siRNA-mediated knockdown**

Synthetic small interfering RNAs (siRNAs) for human and mouse *YAP* and non-targeting siRNAs were purchased from Bioneer (Daejeon, South Korea). Each siRNAs were transfected by electroporation using the Neon Transfection System (Invitrogen, Carlsbad, CA, USA) following the manufacturer's protocol. Briefly, 100 pmol of siRNAs per  $5 \times 10^5$  cells were transfected under the manufacturer's parameters (hBMSCs: 990 V, 40 ms, 1 pulse, 100  $\mu$ l tip; RAW264.7: 1680 V, 20 ms, 1 pulse, 100  $\mu$ l tip). After microporation, cells were transferred to 6-well plates containing complete media without antibiotics. After 48 hours, YAP1 expression levels were determined by Western blot analysis.

### **Mouse femoral fracture model**

All animal experiments were performed in accordance with the Institutional Animal Care and Use Committee (IACUC) and approved by the Yonsei University College of Medicine (No: 2018-0146). The mice were maintained under a 12 hr light/dark cycle,  $22 \pm 2^\circ\text{C}$ , and  $50 \pm 5\%$  humidity. They had *ad libitum* access to food and water. A standardized mid-diaphyseal fracture was induced in ICR mice at eight weeks of age. Mice were anesthetized

with Zoletil (30 mg/kg, Virbac, Carros, France) and Rompun (10 mg/kg, Bayer, Ontario, Canada) by intraperitoneal injection. The left leg was shaved, and an anterior knee incision was made. The vastus lateralis was elevated to expose the femur, and transverse osteotomy was performed. The fractured femur was fixed using a 22-gauge needle. The intramuscular wound and skin incision were closed using nylon suture. Subcutaneous injection of Metacam (1 mg/kg, Boehringer Ingelheim, Ingelheim am Rhein, Germany) was administered immediately following surgery for pain management. Also, mice received pain management until post-surgical day 3. The mice with fractured limbs were randomly divided into the two following groups: vehicle-treated and polaprezinc-treated. Vehicle and polaprezinc (25 mg/kg) were orally administered daily after fracture using a feeding catheter (18G x 37 mm, C1LifeTECH, Cheongju, Chungcheongbuk-do, Korea). Mice were euthanized 21 days post-procedure ( $n = 6$  per group).

#### **Micro-computed tomography ( $\mu$ CT)**

For  $\mu$ CT analysis, femoral samples were fixed in 70% ethanol for 24 hr at room temperature. The fixed samples were analyzed using high-resolution  $\mu$ CT (Skyscan-1173, Skyscan, Kontich, Belgium).  $\mu$ CT image reconstruction and analysis were performed using the reconstruction software NRecon (v1.6.9.8, Skyscan, Kontich, Belgium) and CT-analyzer software CTAn (v1.13.2.1, Skyscan, Kontich, Belgium), respectively. Epiphyseal trabecular bone measuring parameters were analyzed using the 3D model visualization software CT-Vol (v2.0, Skyscan, Kontich, Belgium). The acquisition setting conditions were followed by an X-ray source voltage of 90 kVp and current of 88  $\mu$ A. Beam hardening reduction depended on a 1.0-mm-thick aluminum filter. The pixel size was 7  $\mu$ m, exposure time was 500 ms, the rotation step was 0.3°, with full rotation occurring over 360°. The region of analysis was selected as 5 mm from the proximal to the distal of the fracture midline, which is between the intact cortical of the fracture according to Collier et al<sup>28</sup>. The original cortical bone was excluded from callus analysis using CT-Analyzer software. For determination of callus volume, contoured segmentation was applied to the volume of

interest, and the polar moment of inertia (pMOI) was calculated. The calluses, both including and excluding intact cortical bone, were contoured and stacked by applying a threshold of 255 mg hydroxyapatite/cm<sup>3</sup>. Following the  $\mu$ CT measurements, the samples were prepared for histology.

### **Immunohistochemical analysis**

The femoral samples from each group were fixed in 10% formalin solution for 5–7 days at room temperature. Samples were decalcified in 0.5 M EDTA (pH 7.4) solution for two weeks at room temperature. Decalcified femurs were embedded in paraffin blocks. For paraffin blocks, samples were dehydrated by passage through an ethanol series, cleared twice in xylene, and embedded in paraffin, after which 5  $\mu$ m sections were cut using a rotary microtome. Decalcified femoral sections were stained with hematoxylin and eosin, Masson's trichrome, safranin O and fast green, and TRAP. For histomorphometric quantification, cartilage areas, bone areas, and fibrotic tissue areas of the fracture site were determined by ImageJ software. At least three non-consecutive sections were used for analysis, and the mean value represented one sample. For immunostaining, the sections were deparaffinized, rehydrated, and antigen retrieval was performed using citrate buffer (pH 6.0). Briefly, sections were blocked with 5% FBS in PBST for 1 hr at room temperature and then incubated with anti-osteocalcin (TaKaRa Bio Inc., Shiga, Japan) or anti-YAP1 (Abcam, Cambridge, UK) antibody overnight at 4 °C. After washing in PBST, the samples were incubated with VisUCyte™ HRP polymer antibody (R&D Systems, Minneapolis, MN, USA) for 1 hr at room temperature. Immunoreactive samples were visualized using an AEC substrate kit (Abcam, Cambridge, UK) as described previously<sup>29</sup>. Isotype IgG antibody was used as a negative control. IHC staining was quantified using ImageJ software<sup>30,31</sup>.

### **Immunocytochemistry**

MSCs were seeded at 2,000 cells/cm<sup>2</sup> on 4-well glass chamber slides (Nalge Nunc

International, Rochester, NY, USA), and cells were incubated in 5% CO<sub>2</sub> incubator at 37 °C overnight. After that, cells were washed with PBS, followed by fixation with 4% paraformaldehyde (Sigma-Aldrich, Saint Louis, MO, USA) for 15 min. Permeabilization was accomplished with 0.1% Triton X-100 in PBS for 15 min, followed by blocking with 3% bovine serum albumin (BSA) in PBS for 1 hr. Cells were incubated with a 1:100 dilution of primary antibodies against YAP 1' overnight at 4 °C. After washing three times with PBS, cells were incubated with a 1:500 dilution of primary antibodies against YAP 2' for 1hr. After washing three times with PBS phalloidin (alexa fluor 488, Invitrogen Carlsbad, CA, USA)-conjugated secondary antibodies at a 1:400 dilution in PBS containing 1% BSA for 1 hr at room temperature in the dark. The nuclei were stained with 4',6-diamidino-2- phenylindole (Sigma-Aldrich, Saint Louis, MO, USA), and then examined by LSM780 scanning laser confocal microscope (Zen 2012; Carl Zeiss MicroImaging GMBH, Jena, Germany).

### **Protein fractionation**

The fractionation of cytoplasmic and nuclear extracts was performed using subcellular protein fractionation kit (Thermo scientific, Waltham, MA, USA, 78,840) following the manufacturer's instructions. Briefly, the polaprezinc treated cell pellet was suspended in CER buffer with protease inhibitors and incubated them at 4°C for 10 min. Cytoplasmic extracts were separated by spin down at 4°C at 13000 rpm for 10 min and transferred to new pre-chilled tube. The remained pellet was resuspended in ice-cold NER buffer and incubated on ice for 30 min. Finally, the samples were separated by centrifugation at 4°C at 13,000 rpm for 10 min. The supernatant was collected and used as the soluble nuclear extracts.

### **Statistics and Reproducibility**

Analyses were performed using one-way ANOVA or Student's t-test using GraphPad Prism 6 software. All data are presented as mean  $\pm$  standard deviation for at least three

individual experiments.

Reproducibility. All experiments in this study include at least three biological replicates, and the number of replicates is mentioned in the text or figure legend.

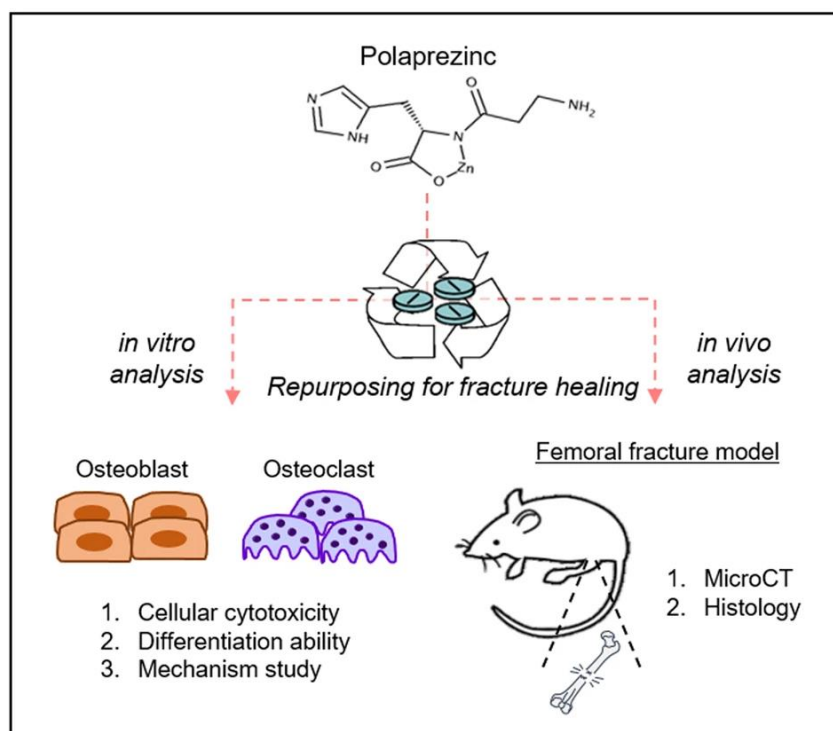
### III. RESULTS

#### **Polaprezinc promotes osteoblast differentiation in hBMSCs**

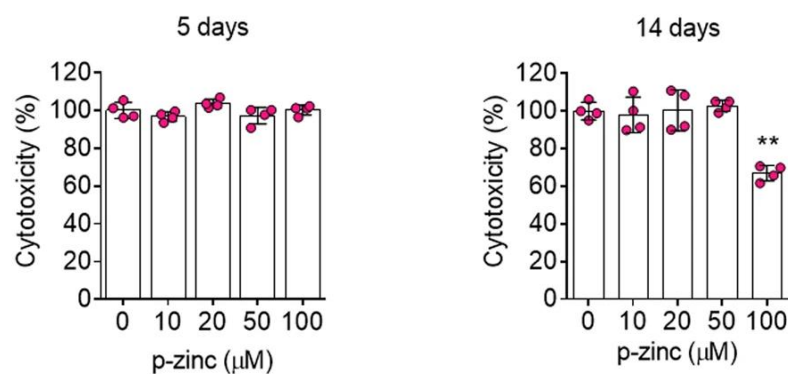
To investigate whether polaprezinc could be a candidate small molecule for drug repurposing to bone-related diseases, we used hBMSCs and mBMMs to determine whether polaprezinc acts as a positive or negative modulator during osteoblast and osteoclast differentiation (**Fig. 1a**). Our previous study showed that zinc sulfate promotes osteoblast differentiation via the PKA-CREB signaling pathway<sup>13</sup>. We wanted to test whether polaprezinc could also act as a positive inducer of the osteogenic differentiation of hBMSCs. Before determining the effect of polaprezinc on osteoblast differentiation, we first tested the cytotoxicity of polaprezinc in hBMSCs. There were no significant differences in cell viability up to five days, but long-term exposure to 100  $\mu$ M of polaprezinc was toxic to hBMSCs (**Fig. 1b**). However, the addition of the same concentration of solvent elicited no cytotoxicity. (However, the addition of 0.5 mM HCl to the culture medium had no cytotoxicity.) Therefore, 50  $\mu$ M of polaprezinc was the most ideal concentration for this study using hBMSCs. Next, we confirmed the effects of polaprezinc on hBMSC differentiation to osteogenic lineage at the early and late stages of differentiation. The results showed that polaprezinc slightly increased ALP activity in the early stage of hBMSC osteogenesis (**Fig. 1c, d**), whereas calcium deposition on the late stage of hBMSC osteogenesis was dose-dependently increased by polaprezinc (**Fig. 1e, f**). Also, we compared the mRNA levels of osteogenic-related genes between vehicle- and polaprezinc-treated hBMSCs. Polaprezinc significantly increased *RUNX2* mRNA levels and downstream genes, such as *ALPL*, *COL1A1*, *SPP1*, *IBSP*, and *BGLAP* (**Fig. 1g**). Consistently, the *RUNX2* protein level was upregulated under polaprezinc treatment, suggesting that polaprezinc might be a positive regulator of hBMSC osteogenesis (**Fig. 1h**).

Therefore, these results indicate that polaprezinc has the potential to enhance hBMSC differentiation into the osteogenic lineage. However, the sole treatment with L-carnosine, one of the compounds chelated in polaprezinc, had no effect on hBMSC osteogenesis (**Fig. 2a-d**).

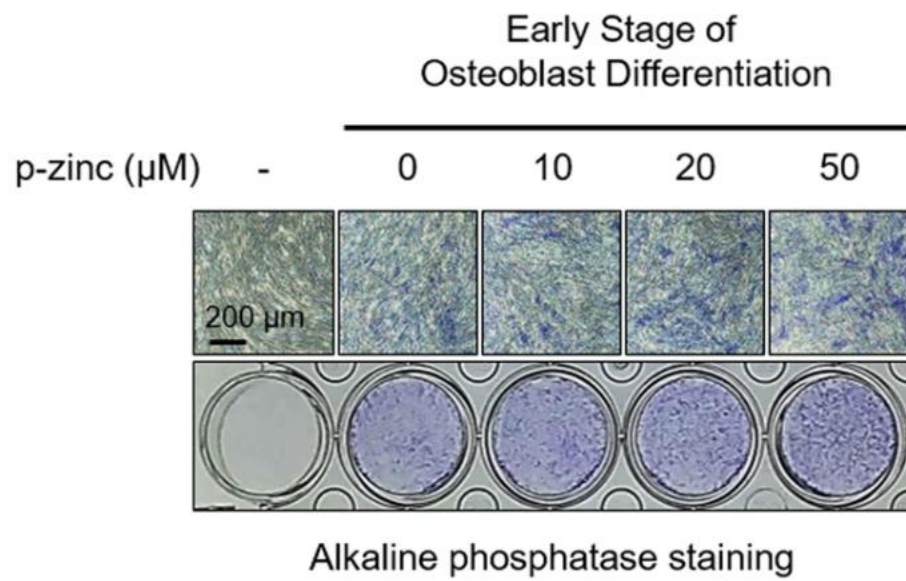
**a**



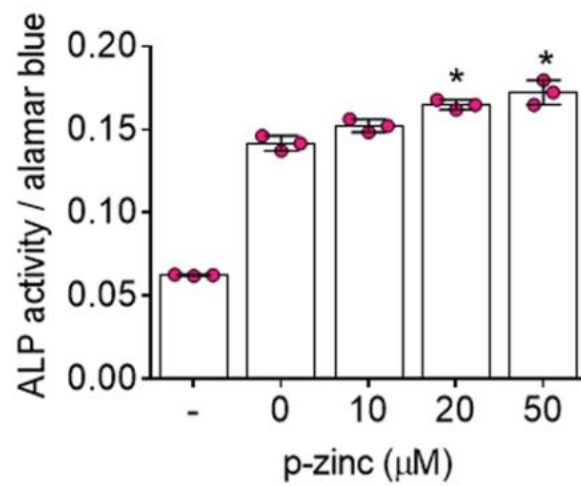
**b**



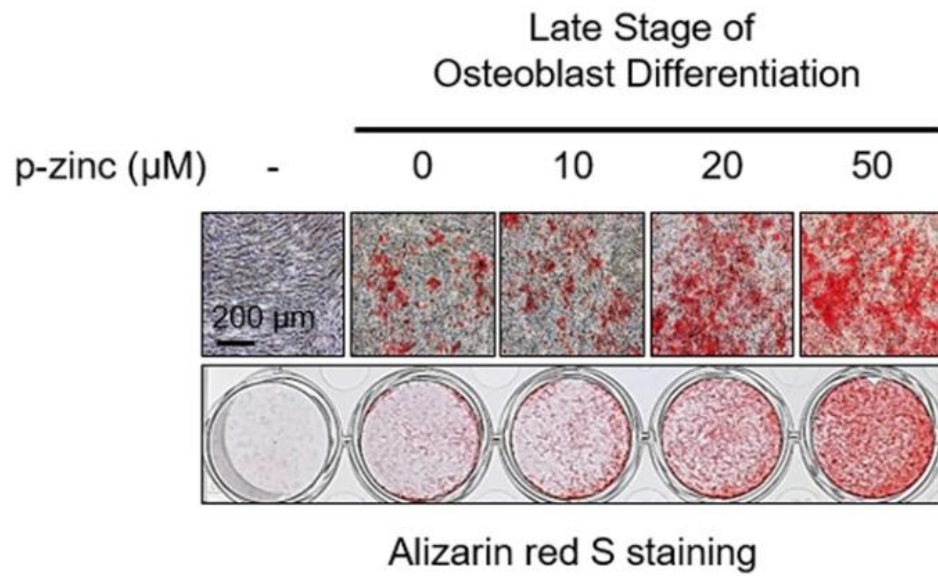
**C**



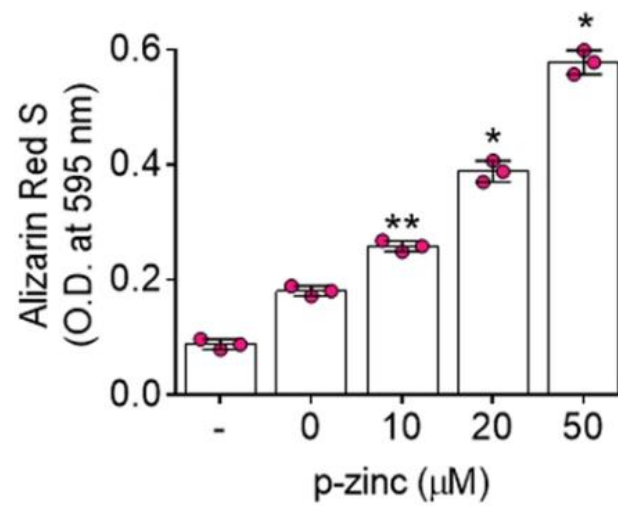
**d**



e



f



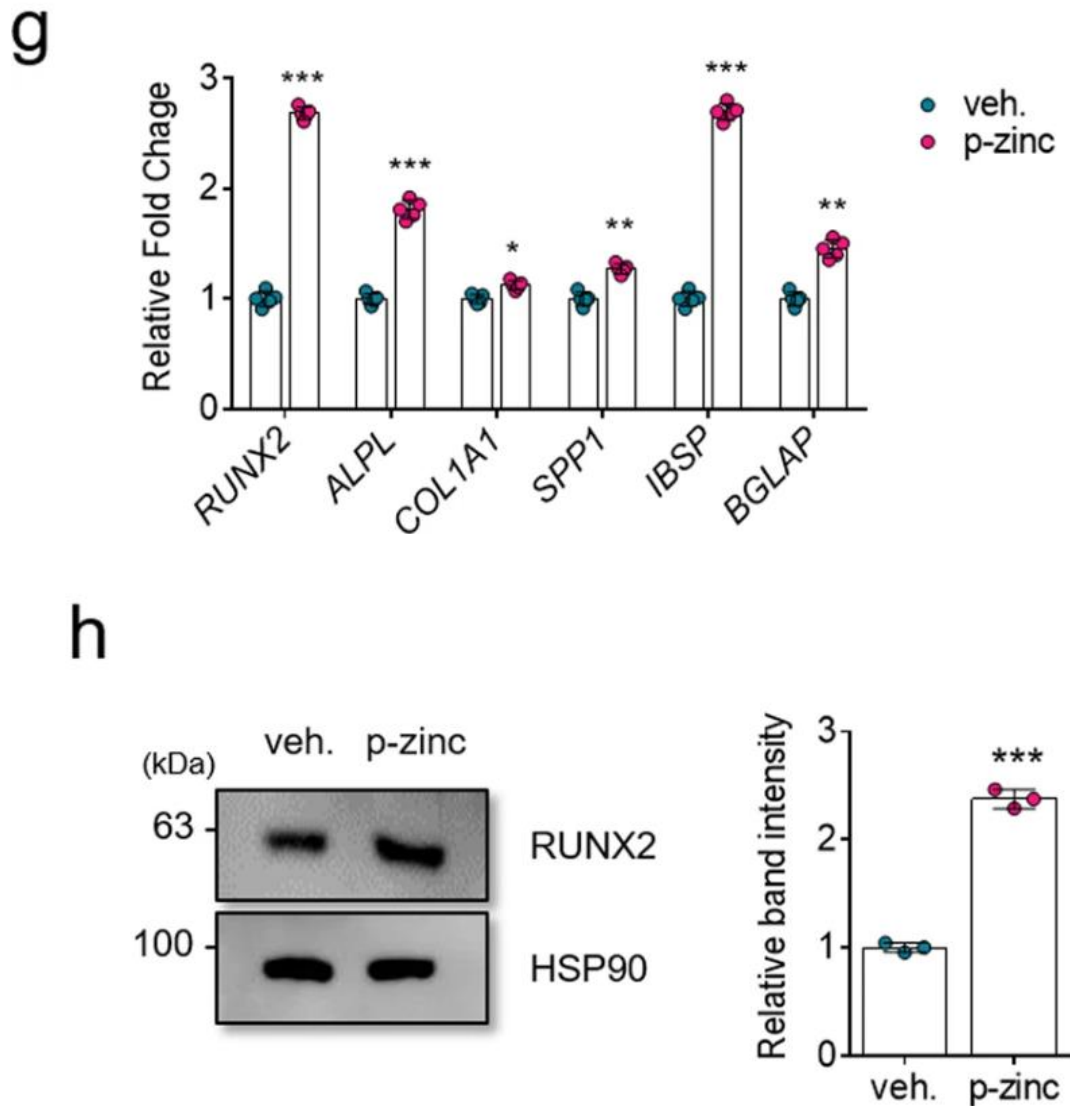
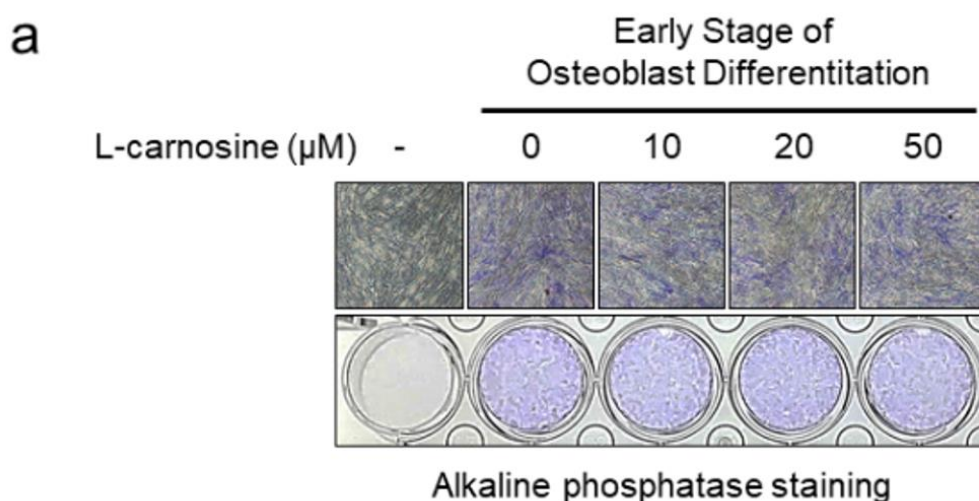
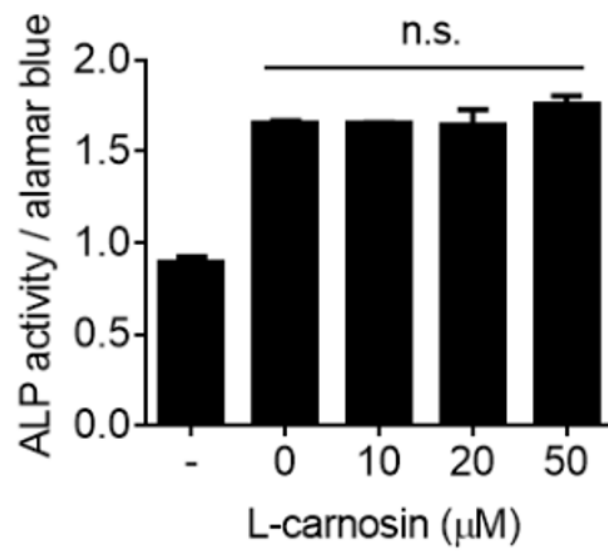


**Figure 1. Schematic of the study and effects of polaprezinc on the osteogenic differentiation of hBMSCs.** (a) Human bone marrow-derived mesenchymal stem cells (hBMSCs) and mouse bone marrow-derived monocytes (mBMMs) were used for *in vitro* studies. For animal studies, ICR mice aged eight weeks were used for further *in vivo* analysis. Polaprezinc was daily administered by oral gavage. (b) The Ez-Cytox assay was used to determine the cellular toxicity of polaprezinc-treated hBMSCs. Each experiment

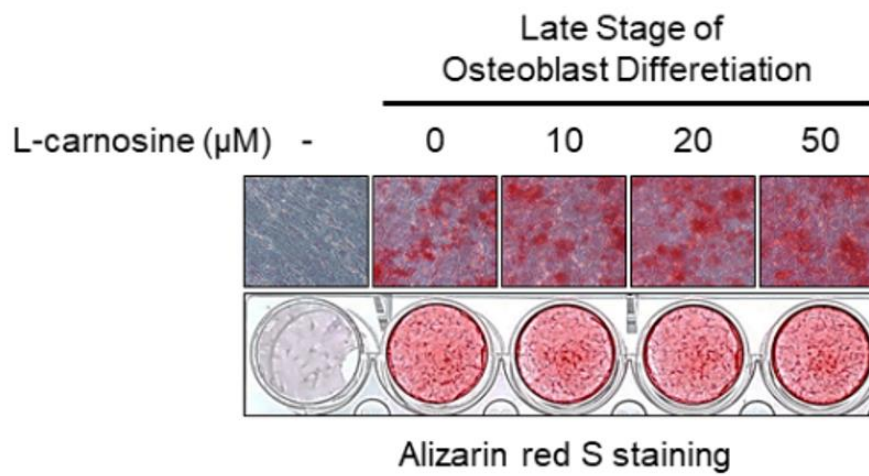
was performed in triplicate ( $n = 3$ ).  $**p < 0.01$  compared with vehicle-treated hBMSCs. (c) Graphs were generated from real-time quantitative PCR data using RNA extracted from hBMSCs treated with polaprezinc (50  $\mu\text{M}$ ) under osteogenic conditions for 3 days. The results were compared to those of the group treated with vehicle ( $n = 3$  experimental replicates). (d) hBMSCs treated with vehicle or polaprezinc (10, 20, and 50  $\mu\text{M}$ ) were incubated in osteogenic medium for seven days. ALP staining was performed to determine the extent of the initial differentiation at day seven. (e) The ALP activity assay was performed for the quantitative analysis of ALP staining. The absorbance was measured at 405 and 450 nm and normalized to that of alamar blue staining. (f) Alizarin red S staining was performed to detect mineral deposition on day 14. (g) For quantitative analysis of alizarin red S staining, absorbance was measured at 595 nm following destaining with 10% cetylpyridinium for 30 min.  $*p < 0.05$  and  $**p < 0.01$  compared with vehicle-treated hBMSCs. (h) The protein level for RUNX2 was analyzed in hBMSCs using western blotting for cells treated with vehicle or polaprezinc (50  $\mu\text{M}$ ) under osteogenic conditions for 5 days. The band intensity was quantified using ImageJ software ( $n = 3$ , in triplicate) and each RUNX2 protein level was normalized to the HSP90 protein level.  $***p < 0.001$  compared with vehicle-treated hBMSCs.

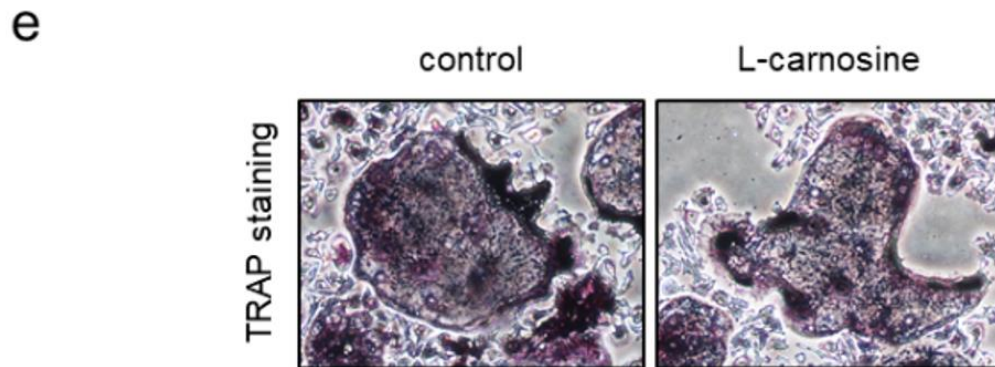
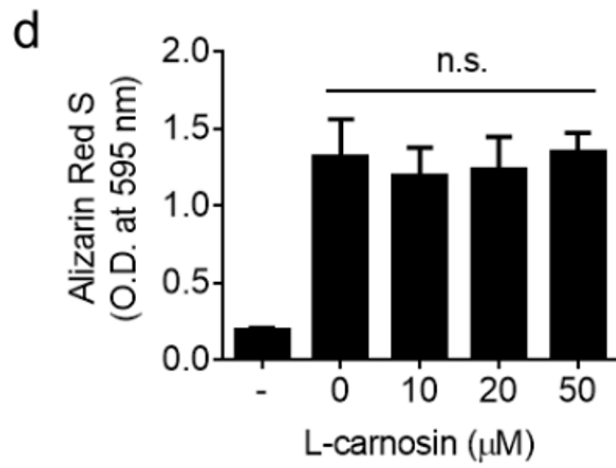


**b**



**c**





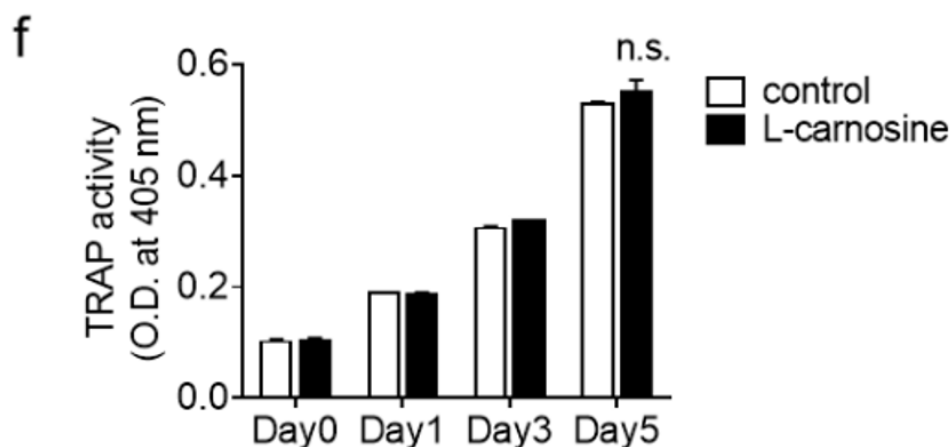
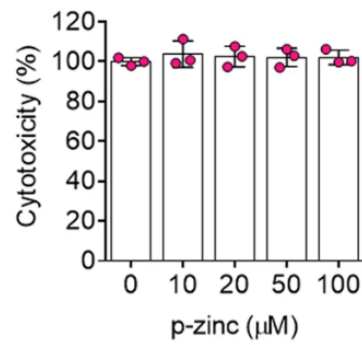


**Figure 2. L-carnosine does not affect osteoblast and osteoclast differentiation.** (a) Mesenchymal stem cells treated with vehicle or L-carnosine (10, 20, and 50  $\mu$ M) were incubated in osteogenic medium for seven days. ALP staining was performed to determine the extent of the initial differentiation at day seven. (b) ALP activity assay was performed for the quantitative analysis of ALP staining. The absorbance was measured at 420 nm and normalized to that of alamar blue staining. (c) Alizarin red S staining was performed to detect mineral deposition at day 14. (d) For quantitative analysis of alizarin red S staining, absorbance was measured at 595 nm following destaining with 10% cetylpyridinium for 30 min. (e) Representative images of osteoclast differentiation. Mouse BMMs treated with vehicle or L-carnosine were seeded in 12-well culture plates and treated for five days with osteoclastogenesis-related reagents (See materials and methods section). TRAP staining was performed to visualize TRAP-positive BMMs. (f) TRAP activity was determined as described in the “materials and methods” section. The absorbance was measured at 405 nm and data are expressed as the mean  $\pm$  S.D. ( $n = 3$ ) from each independent experiment.

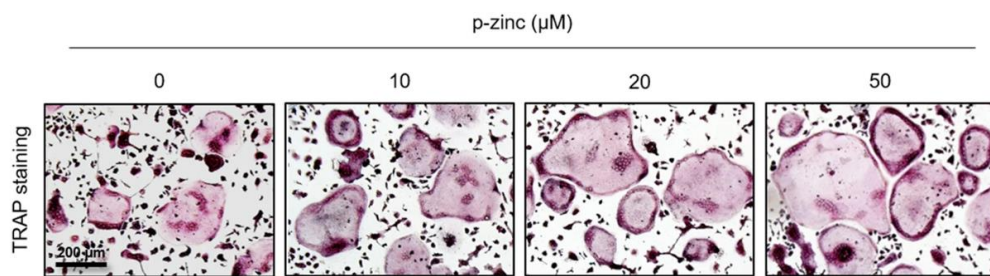
### **Polaprezinc accelerates osteoclast differentiation in mBMMs**

Our previous study showed that osteoclast differentiation was blocked by zinc sulfate treatment in mBMMs<sup>12</sup>; thus, we expected that polaprezinc might have similar effects when compared to previous results regarding zinc. To test this, we first determined the optimal polaprezinc dose by examining the cytotoxic effects of polaprezinc in mBMMs. No cytotoxicity was observed in any of the groups tested for this study (**Fig. 3a**); thus, we used 50  $\mu$ M of polaprezinc, which is same concentration treated in hBMSCs, for further analysis in experiments related to osteoclast differentiation. To clarify the effect of polaprezinc on osteoclast differentiation, mBMMs were induced by treatment with mRANKL in the presence of polaprezinc dose dependently. Unexpectedly, TRAP staining showed that polaprezinc promoted osteoclast formation and fusion (**Fig. 3b**). Consistently, TRAP activity and the number of multinucleated osteoclasts were enhanced by polaprezinc dose dependently (**Fig. 3c, d**), indicating that polaprezinc also acts as a positive regulator of osteoclast differentiation in mBMMs. Furthermore, polaprezinc significantly enhanced mRNA levels of *Nfatc1*, *Ctsk*, and *Dcstamp*, which are critical regulators of osteoclast differentiation<sup>32</sup> in mBMMs (**Fig. 3e**). Consistently, the protein level of NFATc1 was upregulated by polaprezinc treatment (**Fig. 3f**). However, standalone treatment with L-carnosine had no effect on osteoclast differentiation (**Fig. 2e, f**), suggesting that the polaprezinc-mediated enhancement of osteoblast and osteoclast differentiation may be due to the enhanced absorption of zinc by L-carnosine<sup>20,21</sup>.

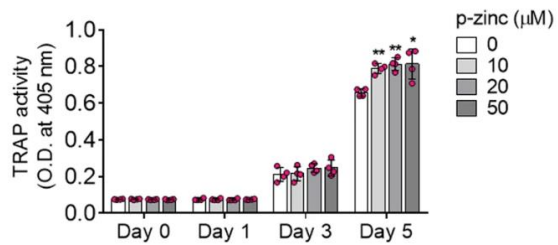
**a**



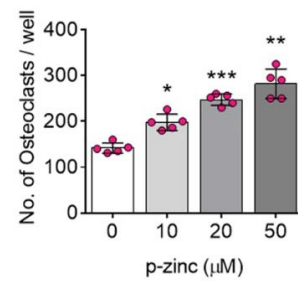
**b**



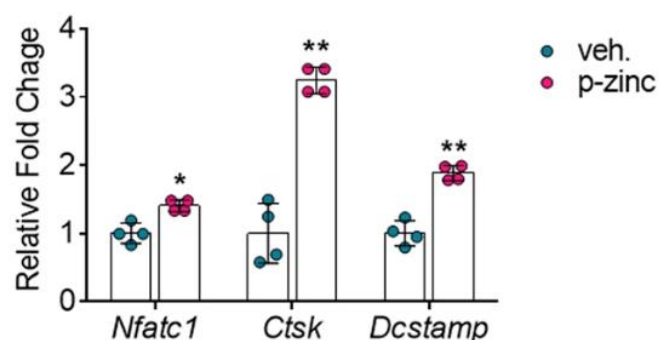
**c**



**d**



e



f

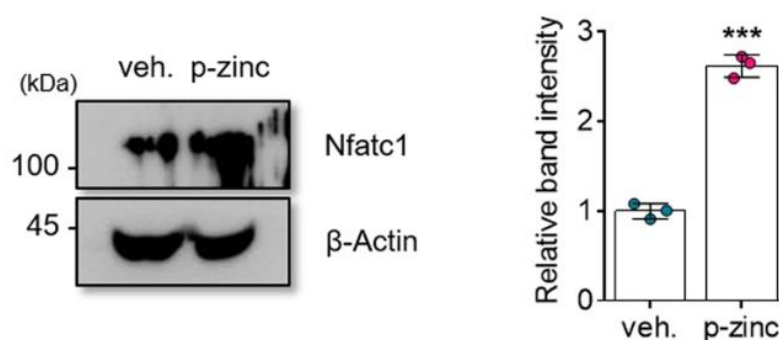
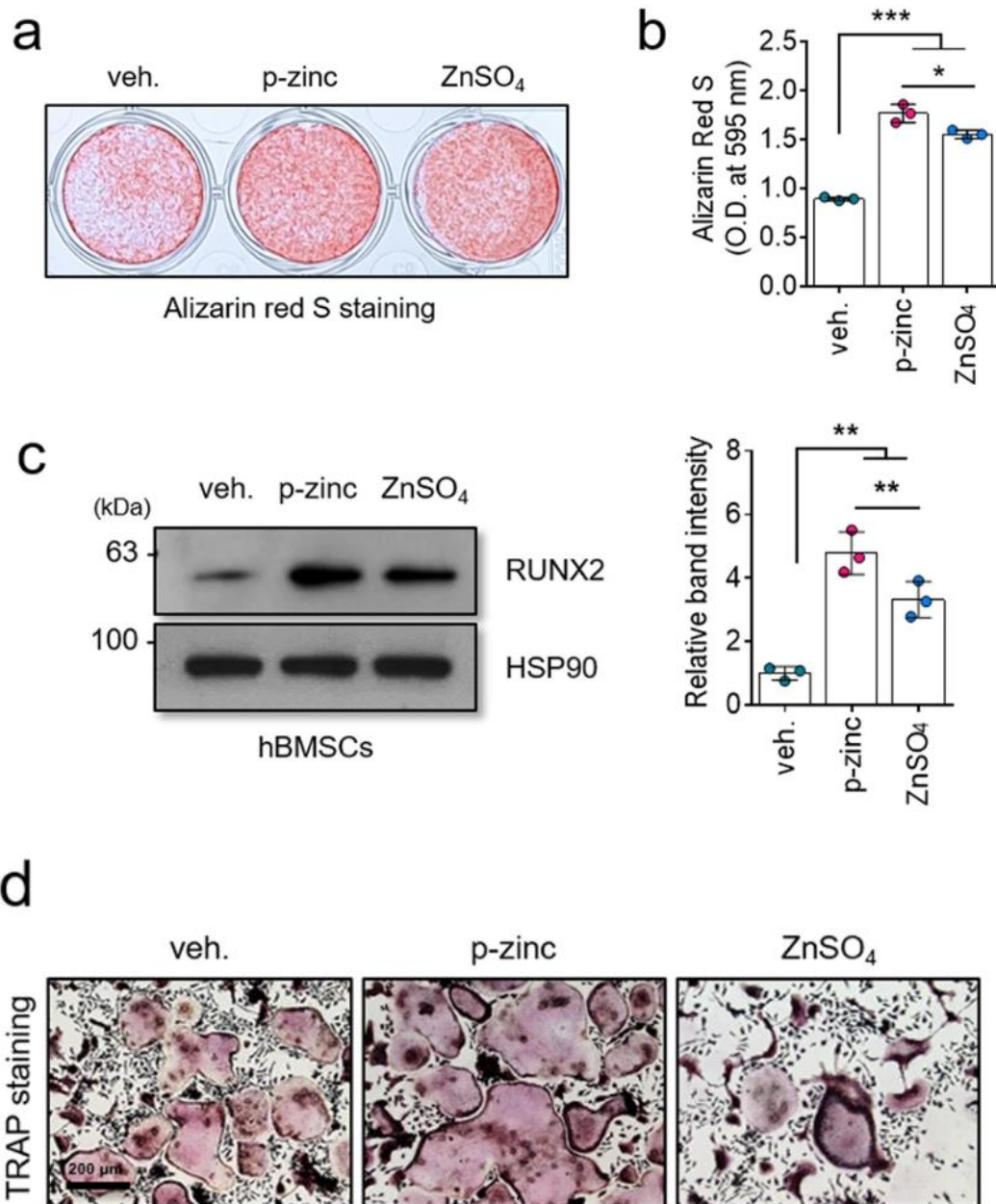


**Figure 3. Effects of polaprezinc on the osteoclast differentiation of mBMMs.** (a) The Ez-Cytox assay was used to determine the cellular toxicity of polaprezinc-treated mBMMs at 5 days. Each experiment was performed in triplicate ( $n = 3$ ). There was no significant difference between groups. (b) Representative images of osteoclast differentiation. mBMMs treated with different concentration of polaprezinc were seeded in 12-well culture plates and treated for five days with 10 ng/mL M-CSF and 10 ng/mL RANKL. TRAP staining was performed to visualize TRAP-positive mBMMs. (c) TRAP activity was determined as described in the materials and methods section. The absorbance was measured at 405 nm and data are expressed as the mean  $\pm$  S.D. ( $n = 3$ ) from each independent experiment. \* $p < 0.05$  and \*\* $p < 0.01$  compared with vehicle-treated mBMMs.

(d) The number of TRAP-positive multinucleated osteoclasts ( $5 \geq$  nuclei) was counted. \* $p < 0.05$ , \*\* $p < 0.01$  and \*\*\* $p < 0.001$  compared with vehicle-treated BMMs. (e) Graphs were generated from real-time quantitative PCR data using RNA extracted from mBMMs treated with polaprezinc (50  $\mu$ M) under osteoclastogenic conditions for 3 days. The results were compared to those of the group treated with vehicle ( $n = 3$  experimental replicates). (f) The protein level for NFATc1 was analyzed in mBMMs using western blotting for cells treated with vehicle or polaprezinc (50  $\mu$ M) under osteoclastogenic conditions for 3 days. The band intensity was quantified using ImageJ software ( $n = 3$ , in triplicate) and each Nfatc1-protein level was normalized to the  $\beta$ -Actin protein level. \*\*\* $p < 0.001$  compared with vehicle-treated mBMMs.

#### **Different effects of polaprezinc and zinc on osteoblast and osteoclast differentiation**

Polaprezinc may have a therapeutic role in bone-related disorders through its dual positive effects on osteoclast and osteoblast differentiation. However, we could not explain the difference in molecular mechanisms between polaprezinc and zinc; this clarification is required since zinc inhibits osteoclast activity<sup>33</sup>. To address the difference between polaprezinc and zinc sulfate, we first tested the effects of polaprezinc and zinc sulfate in osteogenesis. Alizarin red S staining showed that more calcium deposits were present in the polaprezinc-treated group (**Fig. 4a, b**). Also, protein levels of RUNX2 were significantly upregulated in the polaprezinc-treated group, compared to the zinc sulfate group (**Fig. 4c**). In mBMMs, TRAP staining showed that polaprezinc enhanced osteoclast activity, which was decreased in the zinc sulfate group (**Fig. 4d**). Consistently, TRAP activity and the number of multinucleated osteoclasts showed similar results (**Fig. 4e, f**). Moreover, protein levels of NFATc1 were upregulated in the polaprezinc-treated group, but downregulated in the zinc sulfate group (**Fig. 4g**). Additionally, hBMSCs and mBMMs showed no significant differences in zinc absorption between polaprezinc and zinc sulfate (**Fig. 4h**). Thus, we concluded that polaprezinc had a dual positive effect on the differentiation of osteoblasts and osteoclasts, which differed from its role with regular zinc.



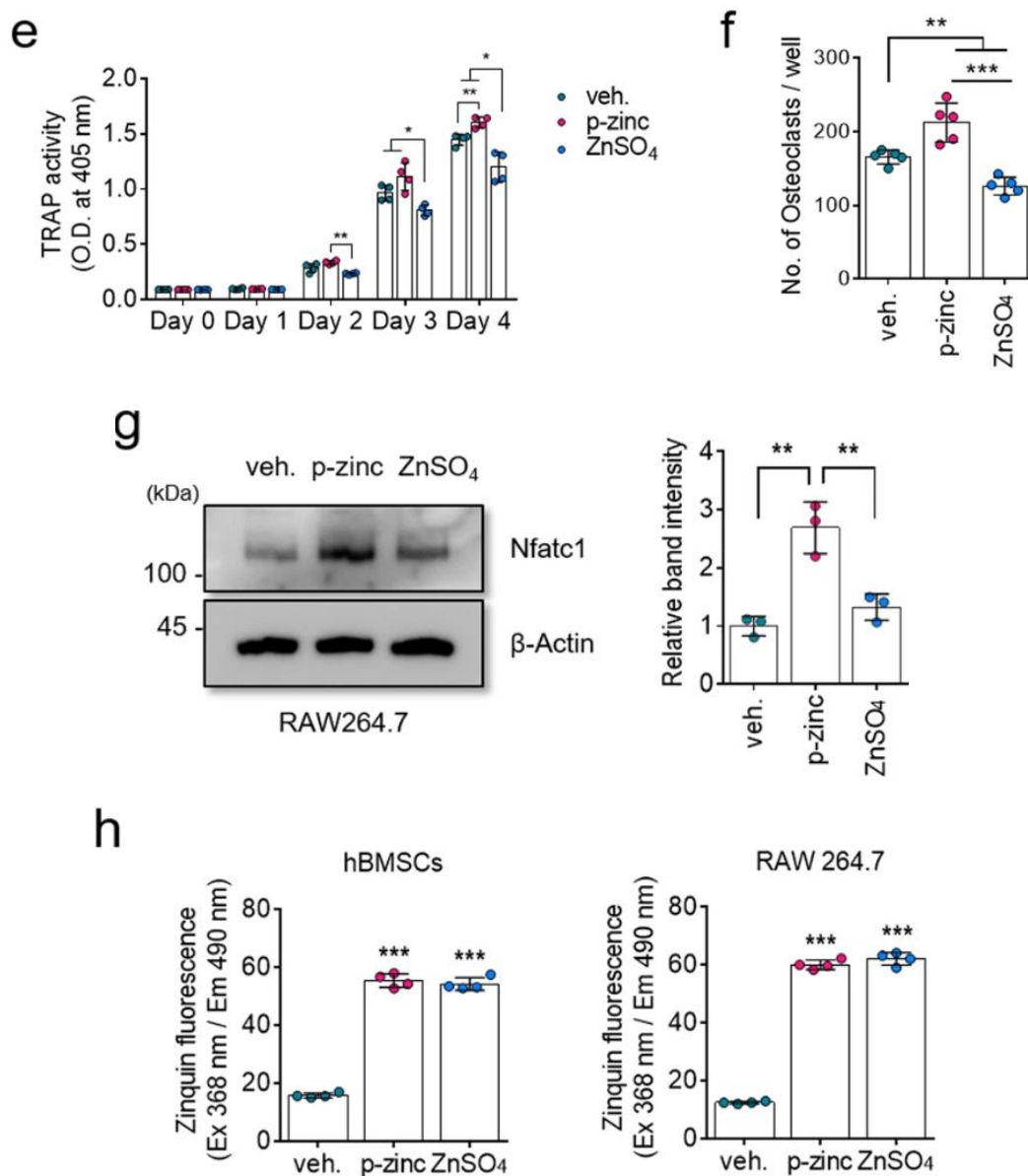


**Figure 4. Comparative study of polaprezinc and zinc sulfate differentiation into osteoblast and osteoclast lineages.** (a) Alizarin red S staining was performed to detect mineral deposition on day 14 in differentiated hBMSCs treated with vehicle, polaprezinc (50  $\mu$ M), or zinc sulfate (50  $\mu$ M). (b) For quantitative analysis of alizarin red S staining,

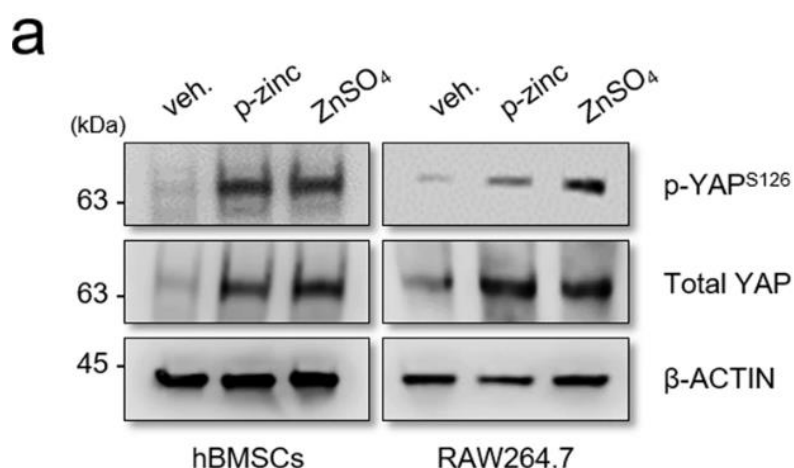
absorbance was measured at 595 nm following destaining with 10% cetylpyridinium for 30 min. (c) The protein level for RUNX2 was analyzed in hBMSCs using western blotting for cells treated with vehicle, polaprezinc (50  $\mu$ M), or zinc sulfate (50  $\mu$ M). The band intensity was quantified using ImageJ software ( $n = 3$ , in triplicate) and each RUNX2 protein level was normalized to the HSP90 protein level. \* $p < 0.05$ , \*\* $p < 0.01$  compared with vehicle-treated hBMSCs. (d) Representative images of osteoclast differentiation. RAW264.7 treated with vehicle, polaprezinc (50  $\mu$ M), or zinc sulfate (50  $\mu$ M) were seeded into 12-well culture plates and treated for five days with osteoclastogenesis-related reagents. TRAP staining was performed to visualize TRAP-positive RAW264.7. (e) TRAP activity was measured at 405 nm, and the data are expressed as the mean  $\pm$  S.D. ( $n = 3$ ) from each independent experiment. (f) The number of TRAP-positive multinucleated osteoclasts ( $5 \geq$  nuclei) was counted. (g) The protein level for NFATc1 was analyzed in RAW264.7 using western blotting for cells treated with vehicle, polaprezinc (50  $\mu$ M) or zinc sulfate (50  $\mu$ M). The band intensity was quantified using ImageJ software ( $n = 3$ , in triplicate) and each Nfatc1 protein level was normalized to the  $\beta$ -Actin protein level. \*\* $p < 0.01$  compared with vehicle-treated RAW264.7. (h) Cells treated with vehicle, polaprezinc (50  $\mu$ M), or zinc sulfate (50  $\mu$ M) were incubated with 25  $\mu$ M of Zinquin for 30 min at 37°C. The fluorescence intensity was measured at excitation 368 nm and emission 490 nm using a fluorometer.

### **YAP may be a responsible molecular mediator of polaprezinc-induced osteoblast and osteoclast activity**

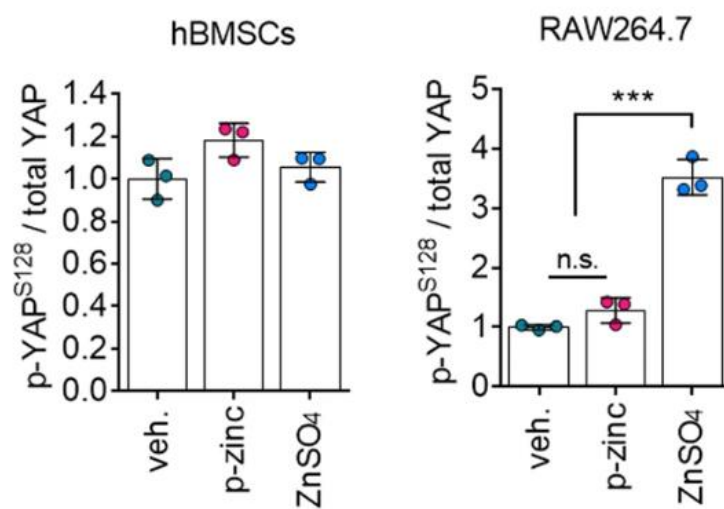
YAP is a transcriptional coactivator that regulates various cellular mechanisms and itself can be regulated during osteoblast and osteoclast differentiation<sup>34,35</sup>. YAP activates the transcription of NFATc1 by interacting with TEAD4 and activator protein-1 (AP-1) to positively regulate osteoclastogenesis<sup>35</sup>. The role of YAP in osteogenesis is controversial in terms of its regulation of RUNX2 activity, but a recent study clarified the ambiguous role of YAP in regulating osteogenesis<sup>36</sup>. They found that YAP can indirectly activate

RUNX2 activity by interacting with AP 2a through a negative feedback mechanism. Overall, YAP has is a common regulator capable of upregulating the activity of the RUNX2 and NFATc1 proteins; thus, we hypothesized that YAP could be responsible for the polaprezinc-mediated upregulation of both proteins. To test this hypothesis, we first observed YAP protein levels in hBMSCs and RAW264.7 cells treated with polaprezinc or zinc sulfate. Interestingly, total YAP protein levels were upregulated in both polaprezinc- and zinc sulfate-treated hBMSCs and RAW264.7 cells (**Fig. 5a**). In hBMSCs, both compounds elevated YAP protein levels, which is consistent with the results of hBMSC osteogenesis enhanced by polaprezinc and zinc sulfate. Both compounds also elevated the protein levels of YAP in RAW264.7 cells treated with polaprezinc and zinc sulfate. However, this result was inconsistent with those of mBMM osteoclastogenesis because upregulation of YAP positively contributes to osteoclastogenesis, as mentioned previously. Thus, we hypothesized that zinc sulfate, unlike polaprezinc, has a different mechanism for regulating the transcriptional activity of the YAP protein on osteoclastogenesis. Phosphorylation of the YAP protein leads to its cytoplasmic retention<sup>37</sup>, thus shutting off nuclear translocation, leading to loss of transcriptional activity regardless of the increase in the amount of protein. Our western blot results regarding YAP phosphorylation may indicate that polaprezinc increased the nuclear localization of YAP protein in RAW264.7 cells, whereas zinc sulfate upregulated YAP phosphorylation (**Fig. 5a, b**). To clarify this, we employed the HOP/HIP flash reporter assay to determine whether polaprezinc affects the transcriptional activity of YAP (**Fig. 5c**). The transcriptional activity of YAP protein in hBMSC was increased in the polaprezinc-treated group and the zinc sulfate-treated group, confirming that both compounds are involved in enhancing the transcriptional activity of the YAP protein (**Fig. 5d**). However, the transcriptional activity of YAP in RAW164.7 cells was increased only in the polaprezinc-treated group (**Fig. 5d**) despite increases in the amount of YAP protein in the zinc-sulfate-treated group (**Fig. 5a**). To address the action mechanism of polaprezinc, which regulates osteoblast and osteoclast differentiation, we performed siRNA-mediated gene knockdown studies targeting YAP. The knockdown

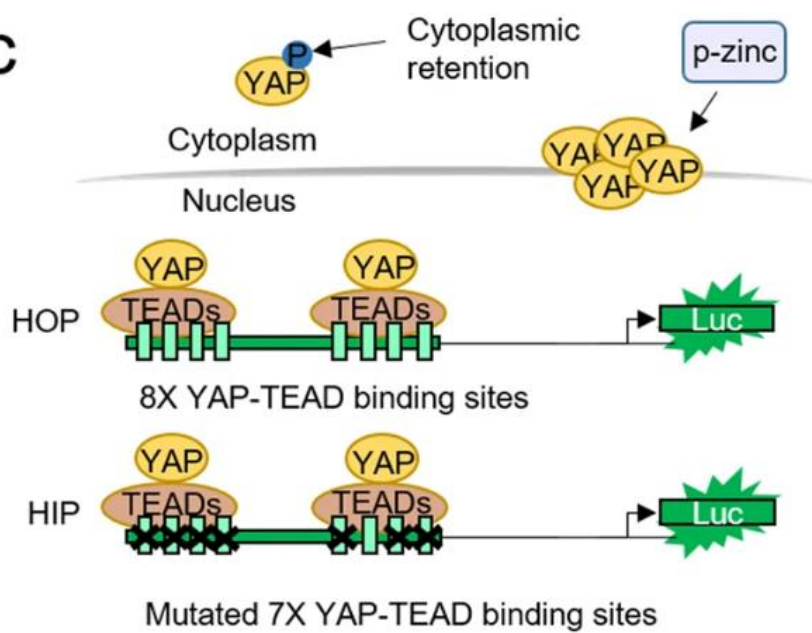
efficiency of YAP was confirmed by Western blot analysis (**Fig. 5e, h**). The siRNA-mediated knockdown of *YAP* suppressed the osteogenic potential of hBMSCs, as well as the enhancement of the polaprezinc-mediated osteogenic potential (**Fig. 5f, g**). Likewise, *YAP* knockdown decreased the osteoclastogenic potential of RAW264.7 cells, and the effect of polaprezinc in the enhanced osteoclast differentiation was abrogated by *YAP* knockdown (**Fig. 5i, j**). Localization of YAP1 was confirmed by polaprezinc treatment in RAW264.7 cells. (**Fig. 5k, l**) Immunofluorescence of YAP and p-YAP after polaprezinc treatment to show nuclear fractionation. Confocal images of nuclear localization of Yap1 protein by polaprezinc treatment. Phalloidin labeling for F-actin (green), immunocytochemistry for Yap1(red) and DAPI labeling for nuclei (blue) were carried out as described in methods. (**Fig. 5k**). Western blot analysis of Yap1 protein level in the nuclear and cytoplasm fraction. LMNB1 and LDH were used as the nuclear and cytoplasm control protein. LNMB1 (lamin B) is the housekeep protein of nucleus, and LDH is the housekeep protein of cytoplasmic protein. (**Fig 5l**) Thus, we concluded that the polaprezinc-mediated enhancement of osteoblast and osteoclast differentiation depends on the presence of YAP, especially in its transcriptional activity.



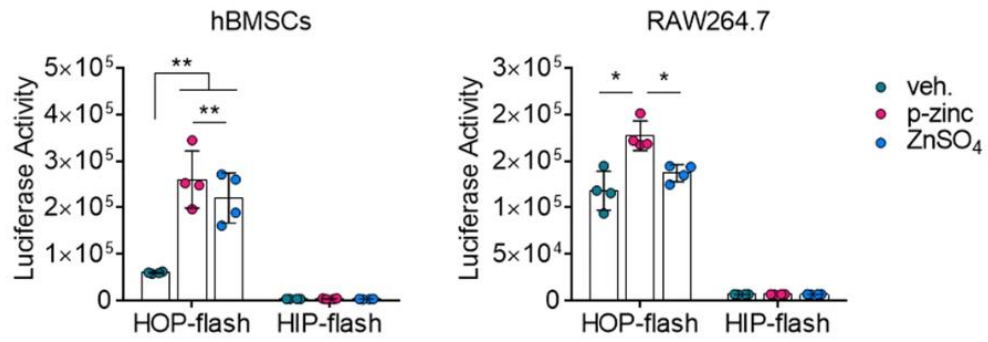
**b**



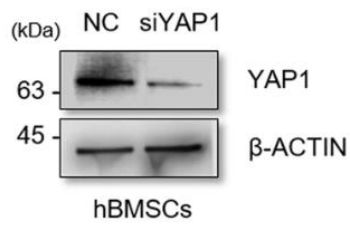
**c**



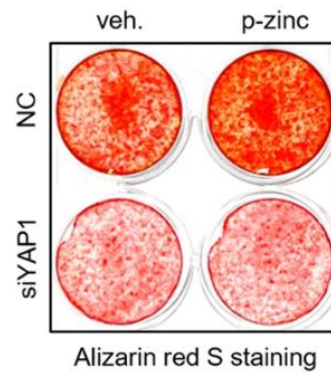
d



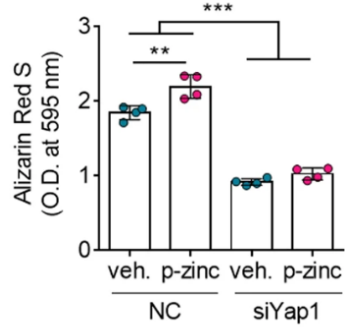
e



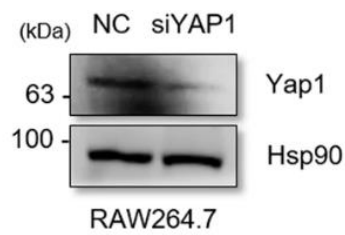
f



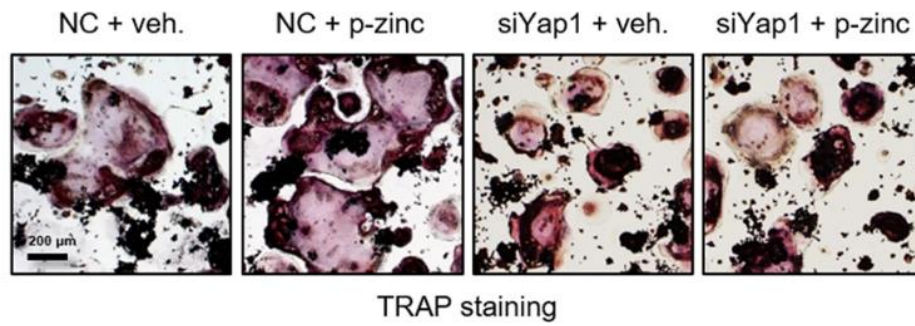
g



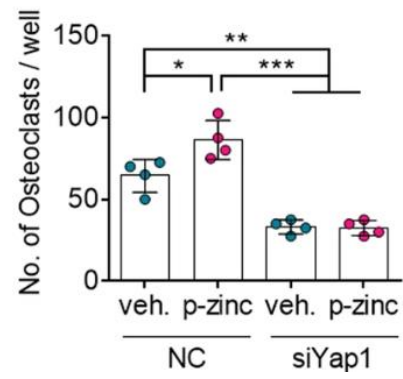
h



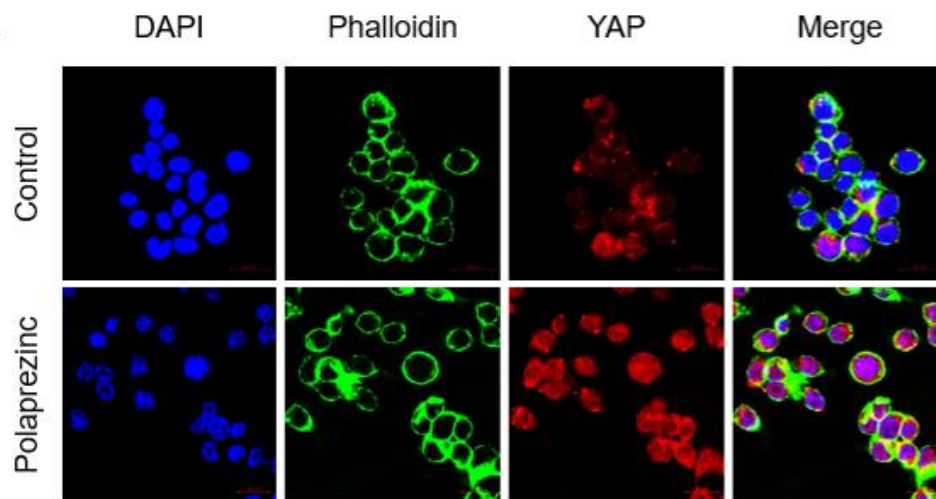
i



j



k



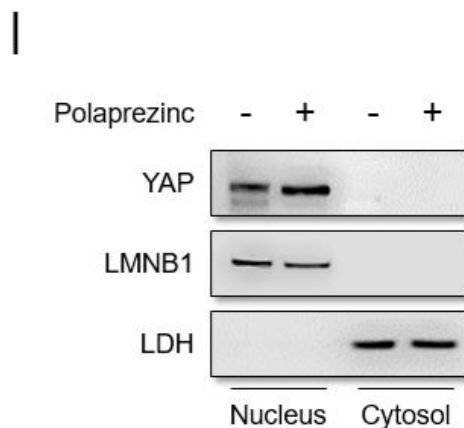


**Figure 5. Knockdown study of YAP in polaprezinc-treated hBMSCs and RAW264.7 cells.**

(a) Protein levels of YAP and phosphorylated YAP<sup>S126</sup> were analyzed in hBMSCs and RAW264.7 cells using western blotting for cells treated with vehicle, polaprezinc (50  $\mu$ M), or zinc sulfate (50  $\mu$ M). (b) The band intensity was quantified using ImageJ software ( $n = 3$ , in triplicate) and the protein level of phosphorylated YAP<sup>S126</sup> was normalized to total YAP protein level. \*\*\* $p < 0.001$  compared with vehicle-treated cells. (c) Schematic of the HOP/HIP flash reporter assay. The HOP luciferase vector has eight YAP-TEAD binding sites whereas seven YAP-TEAD binding sites are mutated in the HIP vector. The quantitative increase of YAP protein by polaprezinc is expected to increase the transcriptional activity of YAP protein. (d) YAP-TEAD transcriptional activity was assessed by luciferase reporter constructs in hBMSCs or RAW264.7. \*  $p < 0.05$ , \*\*  $p < 0.01$ . (e) Western blot analysis of YAP1 protein levels upon transfection with or without *YAP1* siRNA in hBMSCs. (f) Alizarin red S staining was performed to detect mineral deposition on day 14 in negative control or human YAP-targeting siRNA-transfected hBMSCs treated with vehicle or polaprezinc (50  $\mu$ M). (g) For quantitative analysis of alizarin red S staining, absorbance was measured at 595 nm following destaining with 10% cetylpyridinium for 30 min. (h) Western blot analysis of Yap1 protein level transfected with or without *Yap1* siRNA in RAW264.7. (i) Negative control or mouse YAP-targeting siRNA-

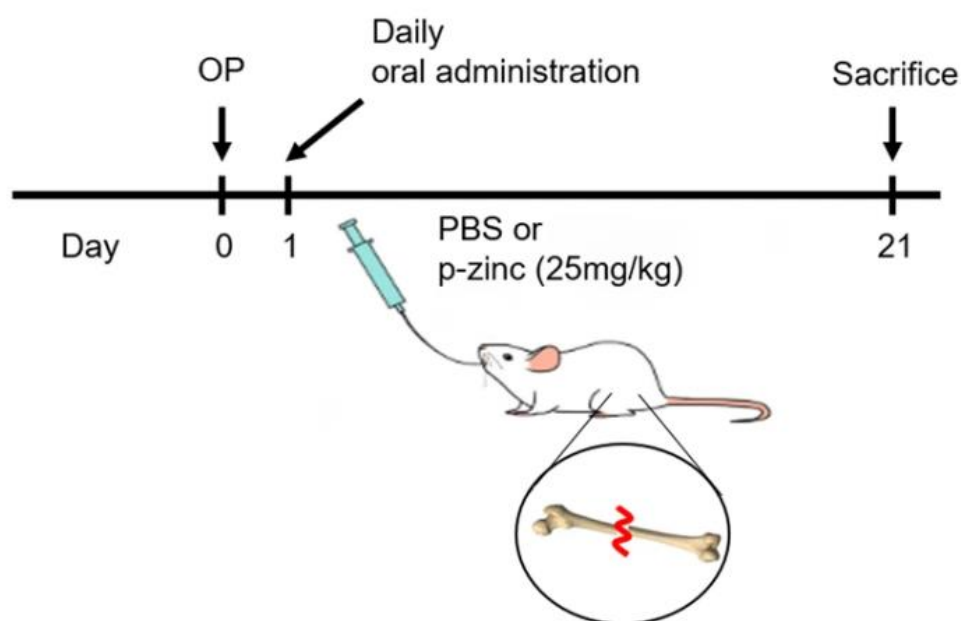
transfected RAW264.7 cells treated with vehicle or polaprezinc (50  $\mu$ M) were seeded into 24-well culture plates and treated for five days with RANKL (50 ng/mL). TRAP staining was performed to visualize TRAP-positive cells. (j) The number of TRAP-positive multinucleated osteoclasts ( $5 \geq$  nuclei) was counted. (k) Confocal images of nuclear localization of Yap1 protein by polaprezinc treatment. Phalloidin labeling for F-actin (green), immunocytochemistry for Yap1 (red) and DAPI labeling for nuclei (blue) were carried out as described in methods. (l) Western blot analysis of Yap1 protein level in the nuclear and cytoplasm fraction. LMNB1 and LDH were used as the nuclear and cytoplasm control protein.

### **Oral administration of polaprezinc accelerates bone remodeling in a mouse fracture model**

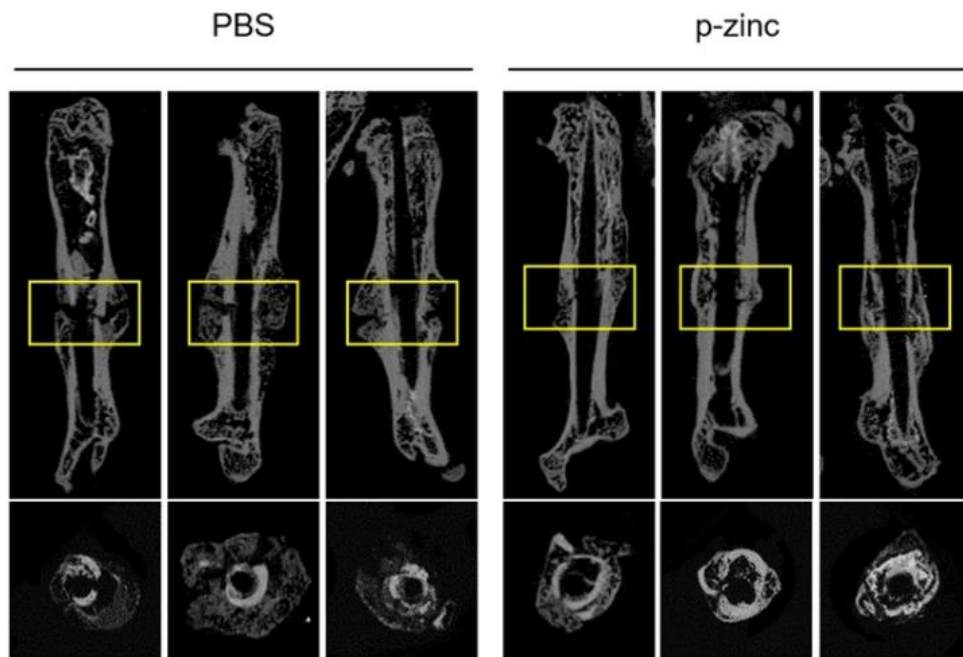
To evaluate whether polaprezinc may serve as a supplement for enhancing the treatment of fracture healing, mice with femoral fractures were employed for animal studies *in vivo*. In a previous study, Yamaguchi et al. reported that oral administration of 25 mg/kg of polaprezinc significantly increased zinc and calcium contents in femoral diaphysis, as well as alkaline phosphatase activity, in weanling rats<sup>38</sup>. We also employed the same dosage of polaprezinc for the current study. From the day after surgery, PBS or polaprezinc was administered daily by oral gavage, and mice were euthanized for further analysis 21 days after surgery (**Fig. 6a**).  $\mu$ CT imaging revealed that the polaprezinc group had lower remaining callus volume than the PBS group (**Fig. 6b**). However, callus bone mineral density (BMD) was significantly increased in the mice orally administered polaprezinc (**Fig. 6c**), indicating that polaprezinc had a positive effect on bone fracture healing. Safranin O staining was conducted to evaluate the osseous calluses formation at the time of euthanasia. The PBS group showed remnant cartilaginous calluses, whereas polaprezinc group showed new bone formation with less cartilage tissue in the fracture areas (**Fig. 6d**), implying that cartilaginous calluses were already replaced by new bone tissue in the mice orally administrated polaprezinc. In quantification of callus regions, cartilage areas and fibrotic tissue areas were significantly reduced; however, bone areas were larger in the polaprezinc group than the PBS group (**Fig. 6e**). These results indicate that polaprezinc promotes cartilage to bone transformation in fractured callus. Next, TRAP staining

was performed to evaluate the number of osteoclasts in the fracture areas. The results showed that the number of osteoclasts increased in the fracture areas of the mice administered polaprezinc (**Fig. 6f, g**). To further investigate the mechanism of accelerated bone healing in the mice administered polaprezinc, we performed immunohistochemistry analysis in fractured calluses. The polaprezinc group showed considerably more osteocalcin protein in the fracture areas of the bone lining cells. Also, YAP was detected in new bone area in the callus and upregulated in the polaprezinc group (**Fig. 6h, i**). These results indicate that oral administration of polaprezinc can induce rapid and successful fracture healing in mice with femoral fractures through active bone homeostasis by multiple osteoblasts and osteoclasts.

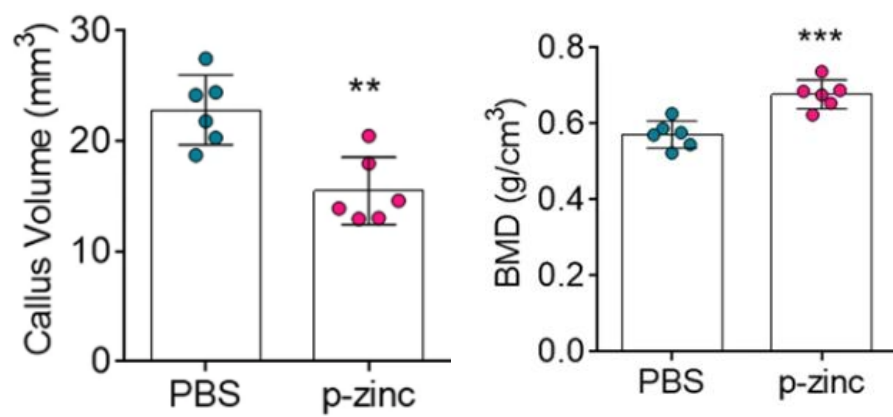
a



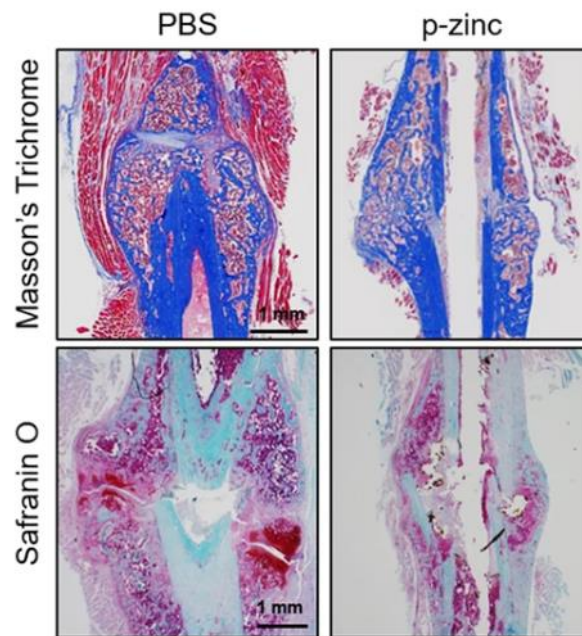
b



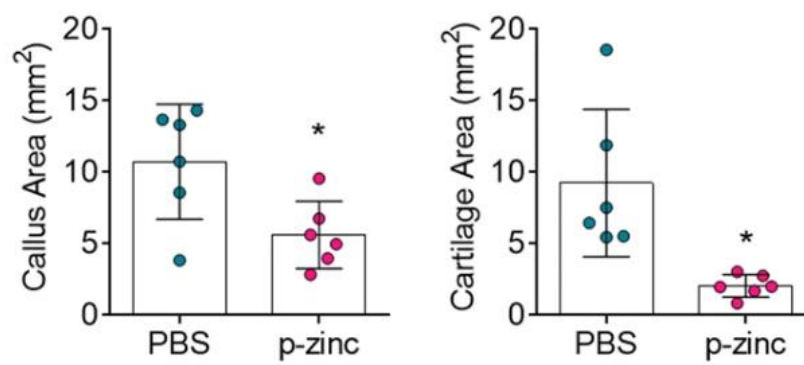
c

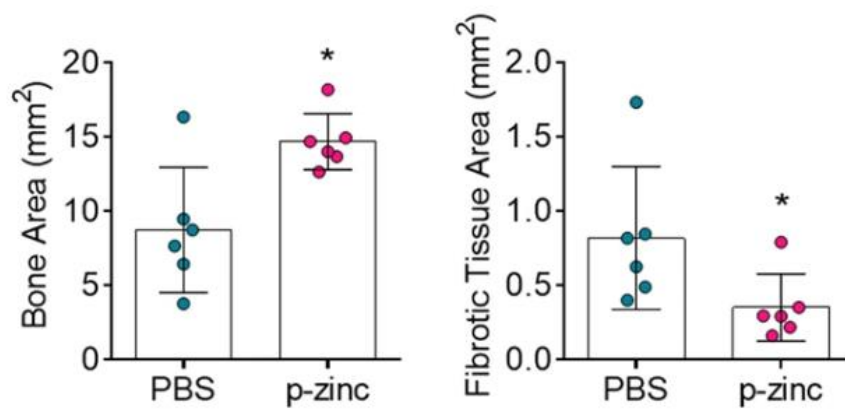


**d**

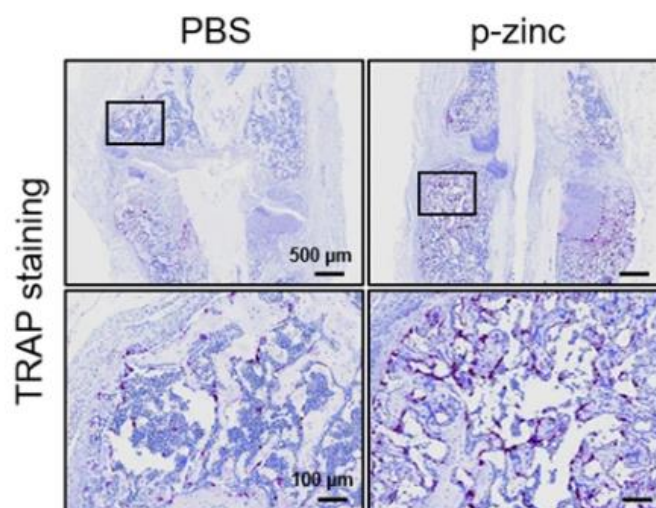


**e**

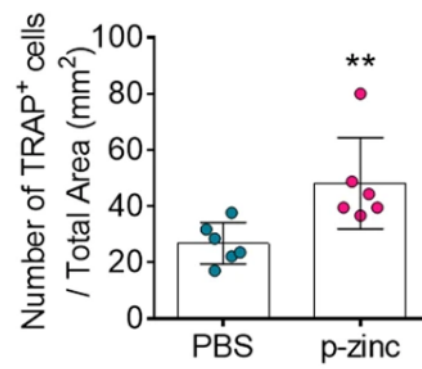




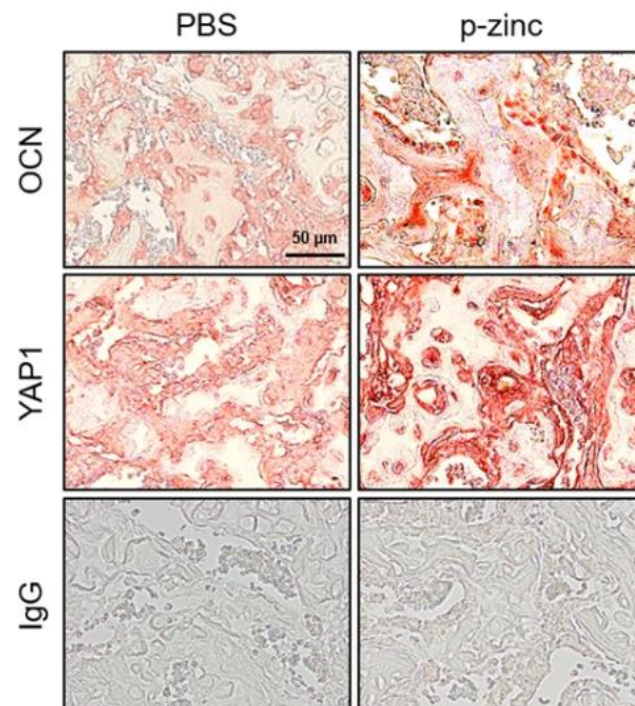
f



g



h



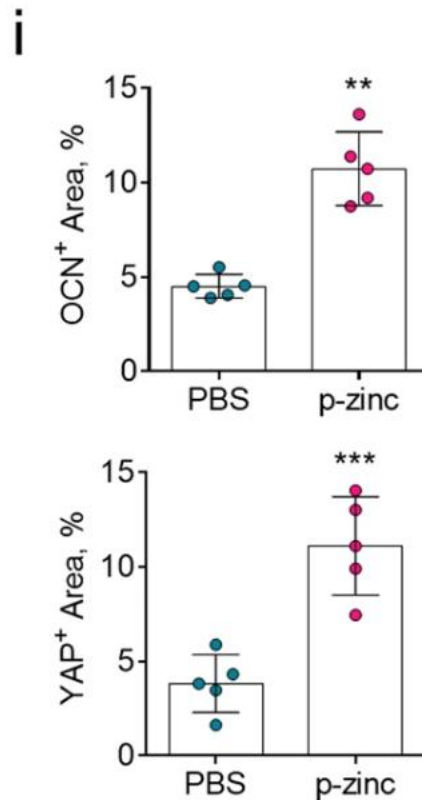


**Figure 6. Micro-CT analysis in a mouse femoral fracture model and the effects of polaprezinc.** (a) Scheme of the animal study. PBS or polaprezinc (25 mg/kg) was orally administered daily after fracture. Mice were euthanized at 21 days post-procedure (n = 6). Femoral samples from each group were collected and subjected to  $\mu$ CT analysis to examine callus formation. (b) Representative  $\mu$ CT images of fracture calluses at three weeks post-closed femur fracture. (c) Callus volume and bone mineral density (BMD) were quantified using  $\mu$ CT analysis. (d) Representative images of the fracture callus stained with safranin O. (e) Quantification of callus area, cartilage area, bone area and fibrotic tissue area. (f) Representative images of the fracture callus stained with TRAP. (g) Quantification of TRAP-positive cells from total cell population per total area ( $\text{mm}^2$ ) in histological sections. (h) Representative images of the fracture callus stained with anti-osteocalcin or anti-YAP1 antibody. (i) Quantification of OCN or YAP positive area by image J software.

#### IV. DISCUSSION

Despite advanced technology and scientific knowledge on treating many types of human diseases, the development of new drugs is extremely expensive and time consuming for such technologies to be applied to patients<sup>39</sup>. These processes place a huge burden on both pharmaceutical companies and patients. Therefore, minimizing time-consuming and costly processes can be a prerequisite for the pharmaceutical industry and inventors. Drug repositioning is a useful strategy for discovering new indications for existing drugs that are inexpensive and risk-free. The development of new drugs involves very complex processes, whereas drug repositioning has only four steps, compound identification, compound acquisition, development, and FDA post-market safety monitoring<sup>40</sup>. Zinc is a useful biomolecule for applications in fracture healing and bone tissue engineering<sup>41</sup>. Nevertheless, there is a need for further studies regarding whether zinc can be used as an effective supplement for bone defect healing in patients with fractures<sup>4,19</sup>. In the fracture healing process, osteoclasts play an important role in the formation of new bones. In this process, the apoptosis of hypertrophic chondrocytes and resorption of the mineralized cartilage matrix by osteoclasts occurs, and is then replaced by new bone at the site of absorption<sup>42-44</sup>. Therefore, the active roles of both osteoblasts and osteoclasts are required for a successful fracture healing process. However, it has long been considered that zinc inhibits the activity of osteoclasts<sup>33,45,46</sup>. If osteoclast activity continues to be suppressed during fracture healing, it can interfere with the normal process of new bone formation. In this regard, polaprezinc is an ideal supplement for patients with fractures.

In the current study, we showed that polaprezinc positively regulates osteoblast and osteoclast differentiation by upregulating mRNA and protein levels of RUNX2 and NFATc1, which are master regulators of osteoblast and osteoclast differentiation<sup>47,48</sup>. This suggests the possibility of using zinc as a novel dual-positive therapeutic agent against bone fracture and other bone diseases. The risk of bone-related diseases is increased by an imbalance in bone resorption and bone formation by osteoclasts and osteoblasts<sup>49</sup>. In the process of bone healing or remodeling, osteoclasts primarily resorb damaged bone,

allowing osteoblasts to further restore the shape and structure of the bone<sup>50</sup>; thus, osteoclasts play a pivotal role during fracture healing. A strategy that disrupts pharmacological osteoclast activity has been used as a therapy for post-menopausal bone loss, but fracture studies using such pharmacological mechanisms in genetic knockout mice have encountered enlarged malformed calluses and persistent fracture gaps<sup>51</sup>, demonstrating the essential role of osteoclasts in soft-callus formation and healing processes. Therefore, maintaining the activity of osteoclasts *in vivo* during fracture healing would be beneficial.

Mechanistically, we proved that polaprezinc treatment induced nuclear localization of YAP protein. Nuclear YAP can initiate NFATc1 transcription by binding AP-1 and TEAD to regulate osteoclastogenesis and related gene expression<sup>35</sup>. In addition, the YAP/RUNX2 axis contributes to successful osteogenesis<sup>52,53</sup>. Recent studies conducted by the Boerckel JD group proved the possibilities of YAP/TAZ as potential therapeutic targets of bone homeostasis and fracture healing. They showed that YAP and TAZ coordinately enhanced osteoblast activity and osteoclast-mediated bone remodeling to promote bone development<sup>54</sup>. In addition, YAP appears to be involved in the expansion and differentiation of periosteal osteoblastic precursor cells in order to promote bone fracture healing<sup>55</sup>. Interestingly, YAP has been shown to be associated with the osteocyte-mediated bone remodeling processes by regulating the mechanical properties of bone matrix organization<sup>56</sup>. Ultimately, evidence from recent studies suggests that YAP-related signaling pathways are deeply connected to skeletal development, as well osteoblast/osteoclast interactions and osteocyte-mediated bone remodeling<sup>57</sup>. Therefore, developing drugs that can specifically activate YAP-related signaling pathways may be a strategy with which to treat bone development- or bone fracture-related injuries. In this study, we showed that zinc or polaprezinc treatment upregulate protein levels of YAP in hBMSCs and RAW264.7 cells. Oral administration of polaprezinc increased YAP-positive cell numbers in the fracture calluses of experimental animals. Considering the results from recent studies, it is clear that zinc is a good candidate for bone homeostasis. Furthermore,

our study demonstrated a relationship between zinc and YAP in osteoblast and osteoclast differentiation. In particular, polaprezinc treatment increased the transcriptional activity of YAP protein in hBMSCs and RAW264.7 cells more than that of the zinc sulfate treatment, although we have not provided detailed mechanisms for how polaprezinc or zinc may be involved in YAP protein increases. Although it may not be an ideal target, it will be partially helpful, and as this study focuses on YAP, various signaling pathways by zinc will definitely help with fracture healing, and YAP will be one of the downstream targets affected by polaprezinc. Nevertheless, the current study is meaningful in that it is the first study to show that polaprezinc is involved in the differentiation of osteoblasts and osteoclasts by enhancing the transcriptional activity of YAP.

## V. CONCLUSION

Polaprezinc promotes osteoblast differentiation in hBMSCs and accelerates osteoclast differentiation in mBMMs. Polaprezinc had a dual-positive effect on the differentiation of osteoblasts and osteoclasts, which differed from its role with regular zinc. Polaprezinc mediated enhancement of osteoblast and osteoclast differentiation depends on the presence of YAP, especially in its transcriptional activity. Oral administration of polaprezinc can induce rapid and successful fracture healing in mice with femoral fractures through active bone homeostasis by multiple osteoblasts and osteoclasts. Our results regarding the effects of polaprezinc on hBMSC osteogenesis and mBMM osteoclastogenesis provide new insights into successful fracture healing by maintaining healthy osteoblasts and osteoclasts throughout. Therefore, we believe that polaprezinc may not only be a supplement for successful fracture healing but also a good candidate for clinical application through drug repositioning.

## REFERENCES

1. Kambe T, Tsuji T, Hashimoto A, Itsumura N. The physiological, biochemical, and molecular roles of zinc transporters in zinc homeostasis and metabolism. *Physiol Rev* 2015;95:749-84.
2. Bergman B, Soremark R. Autoradiographic studies on the distribution of zinc-65 in mice. *J Nutr* 1968;94:6-12.
3. Prasad AS, Halsted JA, Nadimi M. Syndrome of iron deficiency anemia, hepatosplenomegaly, hypogonadism, dwarfism and geophagia. *Am J Med* 1961;31:532-46.
4. O'Connor JP, Kanjilal D, Teitelbaum M, Lin SS, Cottrell JA. Zinc as a therapeutic agent in bone regeneration. *Materials (Basel)* 2020;13.
5. Rondanelli M, Peroni G, Gasparri C, Infantino V, Naso M, Riva A, et al. An overview on the correlation between blood zinc, zinc intake, zinc supplementation and bone mineral density in humans. *Acta Ortop Mex* 2021;35:142-52.
6. Hadley KB, Newman SM, Hunt JR. Dietary zinc reduces osteoclast resorption activities and increases markers of osteoblast differentiation, matrix maturation, and mineralization in the long bones of growing rats. *J Nutr Biochem* 2010;21:297-303.
7. Andruliewicz-Botulinska E, Wisniewska R, Brzoska MM, Rogalska J, Galicka A. Beneficial impact of zinc supplementation on the collagen in the bone tissue of cadmium-exposed rats. *J Appl Toxicol* 2018;38:996-1007.
8. Ryl A, Miazgowski T, Szylińska A, Turon-Skrzypinska A, Jurewicz A,

- Bohatyrewicz A, et al. Bone health in aging men: does zinc and cuprum level matter? *Biomolecules* 2021;11.
9. Cho Y-E, Kwun I-S. Zinc upregulates bone-specific transcription factor Runx2 expression via BMP-2 signaling and Smad-1 phosphorylation in osteoblasts. *J Nutr Health* 2018;51:23-30.
  10. Fukada T, Yamasaki S, Nishida K, Murakami M, Hirano T. Zinc homeostasis and signaling in health and diseases: Zinc signaling. *J Biol Inorg Chem* 2011;16:1123-34.
  11. Nishida K, Hasegawa A, Nakae S, Oboki K, Saito H, Yamasaki S, et al. Zinc transporter Znt5/Slc30a5 is required for the mast cell-mediated delayed-type allergic reaction but not the immediate-type reaction. *J Exp Med* 2009;206:1351-64.
  12. Park KH, Park B, Yoon DS, Kwon SH, Shin DM, Lee JW, et al. Zinc inhibits osteoclast differentiation by suppression of  $Ca^{2+}$ -Calcineurin-NFATc1 signaling pathway. *Cell Commun Signal* 2013;11:74.
  13. Park KH, Choi Y, Yoon DS, Lee KM, Kim D, Lee JW. Zinc promotes osteoblast differentiation in human mesenchymal stem cells via activation of the cAMP-PKA-CREB signaling pathway. *Stem Cells Dev* 2018;27:1125-35.
  14. Palileo C, Kaunitz JD. Gastrointestinal defense mechanisms. *Curr Opin Gastroenterol* 2011;27:543-8.
  15. Ooi TC, Chan KM, Sharif R. Antioxidant, anti-inflammatory, and genomic

- stability enhancement effects of zinc L-carnosine: a potential cancer chemopreventive agent? *Nutr Cancer* 2017;69:201-10.
16. Odawara S, Doi H, Shikata T, Kitajima K, Suzuki H, Niwa Y, et al. Polaprezinc protects normal intestinal epithelium against exposure to ionizing radiation in mice. *Mol Clin Oncol* 2016;5:377-81.
  17. Ooi TC, Chan KM, Sharif R. Zinc carnosine inhibits lipopolysaccharide-induced inflammatory mediators by suppressing NF- $\kappa$ b activation in raw 264.7 macrophages, independent of the MAPKs signaling pathway. *Biol Trace Elem Res* 2016;172:458-64.
  18. Yanagisawa H. Zinc deficiency and clinical practice--validity of zinc preparations. *Yakugaku Zasshi* 2008;128:333-9.
  19. Sadighi A, Roshan MM, Moradi A, Ostadrahimi A. The effects of zinc supplementation on serum zinc, alkaline phosphatase activity and fracture healing of bones. *Saudi Med J* 2008;29:1276-9.
  20. Hewlings S, Kalman D. A review of zinc-L-carnosine and its positive effects on oral mucositis, taste disorders, and gastrointestinal disorders. *Nutrients* 2020;12.
  21. Yoshikawa T, Naito Y, Tanigawa T, Yoneta T, Kondo M. The antioxidant properties of a novel zinc-carnosine chelate compound, N-(3-aminopropionyl)-L-histidinato zinc. *Biochim Biophys Acta* 1991;1115:15-22.
  22. Matsukura T, Tanaka H. Applicability of zinc complex of L-carnosine for medical use. *Biochemistry (Mosc)* 2000;65:817-23.

23. Sano H, Furuta S, Toyama S, Miwa M, Ikeda Y, Suzuki M, et al. Study on the metabolic fate of catena-(S)-[mu-[N alpha-(3- aminopropionyl)histidinato(2-)-N1,N2,O:N tau]-zinc]. 1st communication: absorption, distribution, metabolism and excretion after single administration to rats. *Arzneimittelforschung* 1991;41:965-75.
24. Boldyrev AA, Aldini G, Derave W. Physiology and pathophysiology of carnosine. *Physiol Rev* 2013;93:1803-45.
25. Pushpakom S, Iorio F, Eyers PA, Escott KJ, Hopper S, Wells A, et al. Drug repurposing: progress, challenges and recommendations. *Nat Rev Drug Discov* 2019;18:41-58.
26. Yoon DS, Kim YH, Jung HS, Paik S, Lee JW. Importance of Sox2 in maintenance of cell proliferation and multipotency of mesenchymal stem cells in low-density culture. *Cell Prolif* 2011;44:428-40.
27. Yoon DS, Lee KM, Choi Y, Ko EA, Lee NH, Cho S, et al. TLR4 downregulation by the RNA-binding protein PUM1 alleviates cellular aging and osteoarthritis. *Cell Death Differ* 2022; doi:10.1038/s41418-021-00925-6.
28. Collier CD, Hausman BS, Zulqadar SH, Din ES, Anderson JM, Akkus O, et al. Characterization of a reproducible model of fracture healing in mice using an open femoral osteotomy. *Bone Rep* 2020;12:100250.
29. Yoon DS, Lee KM, Cho S, Ko EA, Kim J, Jung S, et al. Cellular and tissue selectivity of AAV serotypes for gene delivery to chondrocytes and cartilage. *Int J*

- Med Sci 2021;18:3353-60.
30. Crowe AR, Yue W. Semi-quantitative determination of protein expression using immunohistochemistry staining and analysis: an integrated protocol. *Bio Protoc* 2019;9:e3465.
  31. Schneider CA, Rasband WS, Eliceiri KW. NIH Image to ImageJ: 25 years of image analysis. *Nat Methods* 2012;9:671-5.
  32. Kodama J, Kaito T. Osteoclast multinucleation: review of current literature. *Int J Mol Sci* 2020;21:5685.
  33. Moonga BS, Dempster DW. Zinc is a potent inhibitor of osteoclastic bone resorption in vitro. *J Bone Miner Res* 1995;10:453-7.
  34. Pan JX, Xiong L, Zhao K, Zeng P, Wang B, Tang FL, et al. YAP promotes osteogenesis and suppresses adipogenic differentiation by regulating beta-catenin signaling. *Bone Res* 2018;6:18.
  35. Zhao L, Guan H, Song C, Wang Y, Liu C, Cai C, et al. YAP1 is essential for osteoclastogenesis through a TEADs-dependent mechanism. *Bone* 2018;110:177-86.
  36. Lin X, Yang H, Wang L, Li W, Diao S, Du J, et al. AP2a enhanced the osteogenic differentiation of mesenchymal stem cells by inhibiting the formation of YAP/RUNX2 complex and BARX1 transcription. *Cell Prolif* 2019;52:e12522.
  37. Hergovich A. YAP needs Nemo to guide a Hippo. *EMBO Rep* 2017;18:3-4.
  38. Yamaguchi M, Ozaki K. A new zinc compound, beta-alanyl-L-histidinato zinc,

- stimulates bone growth in weanling rats. *Res Exp Med (Berl)* 1990;190:105-10.
39. Scannell JW, Blanckley A, Boldon H, Warrington B. Diagnosing the decline in pharmaceutical R&D efficiency. *Nat Rev Drug Discov* 2012;11:191-200.
  40. Xue H, Li J, Xie H, Wang Y. Review of drug repositioning approaches and resources. *Int J Biol Sci* 2018;14:1232-44.
  41. Oh SA, Kim SH, Won JE, Kim JJ, Shin US, Kim HW. Effects on growth and osteogenic differentiation of mesenchymal stem cells by the zinc-added sol-gel bioactive glass granules. *J Tissue Eng* 2011;2010:475260.
  42. Bronckers AL, Goei W, van Heerde WL, Dumont EA, Reutelingsperger CP, van den Eijnde SM. Phagocytosis of dying chondrocytes by osteoclasts in the mouse growth plate as demonstrated by annexin-V labelling. *Cell Tissue Res* 2000;301:267-72.
  43. Knowles HJ, Moskovsky L, Thompson MS, Grunhen J, Cheng X, Kashima TG, et al. Chondroclasts are mature osteoclasts which are capable of cartilage matrix resorption. *Virchows Arch* 2012;461:205-10.
  44. Shu B, Zhao Y, Zhao S, Pan H, Xie R, Yi D, et al. Inhibition of Axin1 in osteoblast precursor cells leads to defects in postnatal bone growth through suppressing osteoclast formation. *Bone Res* 2020;8:31.
  45. Yamaguchi M. Nutritional factors and bone homeostasis: synergistic effect with zinc and genistein in osteogenesis. *Mol Cell Biochem* 2012;366:201-21.
  46. Yamaguchi M. Role of nutritional zinc in the prevention of osteoporosis. *Mol Cell*

- Biochem 2010;338:241-54.
47. Jensen ED, Gopalakrishnan R, Westendorf JJ. Regulation of gene expression in osteoblasts. *Biofactors* 2010;36:25-32.
  48. Kim JH, Kim N. Regulation of NFATc1 in osteoclast differentiation. *J Bone Metab* 2014;21:233-41.
  49. Feng X, McDonald JM. Disorders of bone remodeling. *Annu Rev Pathol* 2011;6:121-45.
  50. Bahney CS, Zondervan RL, Allison P, Theologis A, Ashley JW, Ahn J, et al. Cellular biology of fracture healing. *J Orthop Res* 2019;37:35-50.
  51. He LH, Liu M, He Y, Xiao E, Zhao L, Zhang T, et al. TRPV1 deletion impaired fracture healing and inhibited osteoclast and osteoblast differentiation. *Sci Rep* 2017;7:42385.
  52. Yang JX, Xie P, Li YS, Wen T, Yang XC. Osteoclast-derived miR-23a-5p-containing exosomes inhibit osteogenic differentiation by regulating Runx2. *Cell Signal* 2020;70:109504.
  53. Kovar H, Bierbaumer L, Radic-Sarikas B. The YAP/TAZ pathway in osteogenesis and bone sarcoma pathogenesis. *Cells* 2020;9:972.
  54. Kegelman CD, Mason DE, Dawahare JH, Horan DJ, Vigil GD, Howard SS, et al. Skeletal cell YAP and TAZ combinatorially promote bone development. *FASEB J* 2018;32:2706-21.
  55. Kegelman CD, Nijsure MP, Moharrer Y, Pearson HB, Dawahare JH, Jordan KM,

- et al. YAP and TAZ promote periosteal osteoblast precursor expansion and differentiation for fracture repair. *J Bone Miner Res* 2021;36:143-57.
56. Kegelman CD, Coulombe JC, Jordan KM, Horan DJ, Qin L, Robling AG, et al. YAP and TAZ mediate osteocyte perilacunar/canalicular remodeling. *J Bone Miner Res* 2020;35:196-210.
57. Kegelman CD, Collins JM, Nijsure MP, Eastburn EA, Boerckel JD. Gone caving: roles of the transcriptional regulators yap and taz in skeletal development. *Curr Osteoporos Rep* 2020;18:526-40.

## ABSTRACT (IN KOREAN)

## 파골세포와 조골세포의 분화 및 골절 치유에서 폴라프레징크의 역할

&lt;지도교수 이 진 우&gt;

연세대학교 대학원 의학과

박 유 정

서론: 골절과 골절 관련 합병증은 최근 가장 흔한 질병 및 사망의 원인 중 하나이다. 국민건강보험공단 자료에 따르면 한국에서는 남녀노소를 불문하고 매년 220만 건 이상의 골절이 발생하고 있다. 대다수가 만족스럽게 치유되지만 5~10%는 지연유합 또는 불유합으로 진행된다. 비타민 D와 칼슘은 골절 치료에 널리 사용되는 보충제이며, 아연 역시 건강한 뼈를 위한 영양 보충제로 인식되어 왔다. 본 연구에서는 골절 치유를 위한 치료제로서 아연과 L-카르노신의 킬레이트 형태의 약물인 폴라프레징크를 골절의 치료제로서 사용 가능한지를 알아보고자 하였다.

방법: 폴라프레징크가 골절의 치료제로서 약물 재배치의 좋은 후보가 될 수 있는지를 알아보기 위해, 인간 골수 유래 중간엽 줄기세포와 생쥐 골수 유래 단핵구를 사용하여 폴라프레징크가 조골세포와 파골세포 분화 동안 양의 조절제 또는 음의 조절제로 작용하는지 여부를 관찰하였다. 다음으로, 분화 초기 및 후기 단계에서 인간 골수 유래 중간엽 줄기세포 분화에서 골형성 계통으로의 폴라프레징크 영향을 관찰하였다.

폴라프레징크로 처리된 인간 골수 유래 중간엽 줄기세포와 대조군 간의 골형성 관련 유전자의 mRNA 수준을 비교했다. 파골세포 분화에 대한 폴라프레징크의 영향을 명확히 하기 위해 생쥐 골수 유래 단핵구는 mRANKL로 처리하여 폴라프레징크의 양을 다르게 하여 유도하였다. 폴라프레징크가 골절 치료제로서의 역할을 할 수 있는지를 평가하기 위해 대퇴골 골절이 있는 쥐를 동물 연구에 사용하였다.

결과: 폴라프레징크는 인간 골수 유래 중간엽 줄기세포에서 조골세포 분화를 촉진하고, 생쥐 골수 유래 단핵구에서 파골세포 분화를 촉진하였다. 즉, 조골세포와 파골세포의 분화에 이중양성 효과를 보였는데, 이는 일반 아연의 역할과는 차이가 있었다. 폴라프레징크의 조골세포 및 파골세포 분화는 특히 전사 활성화에서 YAP의 존재에 따라 달라졌다. 폴라프레징크를 경구 투여하면 다수의 조골세포와 파골세포에 의한 능동적인 뼈 항상성을 통해 대퇴골 골절이 있는 쥐에게 신속하고 성공적인 골절 치유를 유도할 수 있었다.

결론: 폴라프레징크는 조골세포와 파골세포의 활성을 향상시켜 골절 치유 과정을 효율적으로 촉진한다. 따라서, 우리는 폴라프레징크가 성공적인 골절 치유를 위한 치료제일 뿐만 아니라 약물 재배치를 통해 임상 적용에 좋은 후보가 될 수 있다고 생각한다.

핵심되는말: 폴라프레징크, 골절 치유, 약물 재배치, 조골세포, 파골세포

## PUBLICATION LIST

1. Ko EA, Park YJ, Yoon DS, Lee K-M, Kim J, Jung S, et al. Drug repositioning of polaprezinc for bone fracture healing. *Communications Biology*. 2022;5:462-73.